HAL open science

Ion-induced electron emission by keV-range energy indium ions: Influence of material and geometry

V. Hugonnaud, Stéphane Mazouffre, D. Krejci

▶ To cite this version:

V. Hugonnaud, Stéphane Mazouffre, D. Krejci. Ion-induced electron emission by keV-range energy indium ions: Influence of material and geometry. Journal of Applied Physics, 2022, 132 (19), pp.193302. 10.1063/5.0102206 . hal-03891291

HAL Id: hal-03891291

https://cnrs.hal.science/hal-03891291v1

Submitted on 16 Nov 2023

HAL is a multi-disciplinary open access archive for the deposit and dissemination of scientific research documents, whether they are published or not. The documents may come from teaching and research institutions in France or abroad, or from public or private research centers.

L'archive ouverte pluridisciplinaire **HAL**, est destinée au dépôt et à la diffusion de documents scientifiques de niveau recherche, publiés ou non, émanant des établissements d'enseignement et de recherche français ou étrangers, des laboratoires publics ou privés.

Public Domain

ACCEPTED MANUSCRIPT
This is the author's peer reviewed, accepted manuscript. However, the online version of record will be different from this version once it has been copyedited and typeset.
PLEASE CITE THIS ARTICLE AS DOI: 10.1063/5.0102206
Journal of Applied Physics
AIP Publishing

Ion-induced electron emission by keV-range energy indium ions: Influence of material and geometry.

V.Hugonnaud,[1, 2, a)] S.Mazouffre,[2, b)] and D.Krejci[1, c)]
[1)] *Enpulsion, Viktor kaplan straße 2700, Wiener Neustadt, Austria*
[2)] *CNRS-ICARE, 3 Avenue de la Recherche Scientifique, 45100 Orléans, France*

(Dated: 13 October 2022)

This work provides measurements of the ion-induced electron emission (SEE) yield caused by keV-range energy indium ions (3 to 8 keV). In our experiment the ion sources, fuelled with indium, are based on the working principle of field-emission electric propulsion (FEEP) technologies. The measured yields are given for different material properties (plain structure vs foam) and geometries (flat surface vs conical). Study outcomes show that electrons induced by keV-range indium ions can lead to overestimate the measured ion current by 30% to 200% depending on the collector materials and geometry. We spotlighted that molybdenum, tungsten and stainless steel 316L have relatively low yields compared to aluminium 2017A. Moreover, it is possible to lower down a specific material yield by two third when using a foam structure. Finally, it is shown that off-axis ions influence on a collector increase the resulting electron emission yield. In the case of an indium-FEEP thruster ion-induced electron emissions are a major perturbation when measuring ion current. Mainly due to the energy range of ions studied, yields retrieved are orders of magnitudes larger than what it is usually measured when studying the plume of an electrostatic electric propulsion system. It is therefore strongly recommended to use a so-called Faraday cup to study the ion beam from an indium-FEEP thruster as the probe close architecture allows to greatly mitigate these perturbations.

I. INTRODUCTION

Over the last decade the demand in electric propulsion (EP) systems has increased. Therefore, plume characterisation by mean of electrostatic probes is a subject of interest as it provides meaningful information on thruster performances and plume-spacecraft interaction. Electrostatic probes are often used to measure plasma properties within the plume created by an electric thruster[1–4]. Probe types are numerous[1,2,5–15] and enable acquisition of current density, particles energy and velocity. To enhance probe current collection efficiency, designs have evolved to sophisticated architecture using systems of electrode or close geometry structure[12,13]. Despite many effects, current measurement accuracy still depends largely on the collector material, the probe geometry and the plasma properties. Ion-induced electron emission (SEE) is a fundamental surface interaction which can strongly influence the total ion current measured by the device. Lately, strong interest from satellite manufacturers in electric thrusters using molten metal indium as propellant spotlighted scarce data availability of electrons induced by keV-range energy indium ion bombardment. Consequently, we propose in this study to experimentally measure the yield of ion-induced electrons (γ_{SEE}) emitted by different materials when bombarded by energetic (3 keV to 8 keV) indium ions. γ_{SEE} is given for aluminium 2017A, stainless steel 316L, tungsten and molybdenum for an ion beam incidence normal to the material surface. To this end, we updated the design of an electrostatic probe termed Faraday cup (FC)[11,16,17] to properly measure the yield. A FC is a well known device which measures electron or ion currents when the collector is biased positively or negatively, respectively. γ_{SEE} is also measured for different ion collector shapes modifying the ion beam incidence angle.

[a)] Author to whom correspondence should be addressed: valentin.hugonnaud@enpulsion.com
[b)] stephane.mazouffre@cnrs-orleans.fr
[c)] david.krejci@enpulsion.com

II. EXPERIMENTAL APPARATUS

A. Test bench, mechanical interface and instrument

Measurements were done in a cylindrical stainless-steel vacuum vessel of 0.91 m in diameter and 1.75 m in length located at the aerospace engineering's department laboratory of Wiener Neustadt University of Applied Sciences (FH Wiener Neustadt). During operation the pressure level typically was 2×10^{-6} mbar. The chamber frame is connected to ground which is the voltage reference for this study.

An aluminium rotating arm allows automatic alignment of the probe with the thruster equatorial plane. The probe holder is mounted on a URS1000BCC motorized rotation stage from Newport. A Newport's SMC100 enables to control the motor from the atmospheric side. The thruster centreline is referred to as the 0 angular position. The pivot point of the rotating structure is aligned with the thruster exit plane. The system enables a scan from -90 to +90 in the horizontal plane with respect to the thruster. The distance R between the FC aperture and the thruster exit plane is 25.5 cm. The entire mechanical structured is grounded. Further description can be found here[18].

A calibrated Keithley 2050 sourcemeter is used to measure the ion current. The device is operated in voltage source and measures current with 0.012% basic accuracy.

ACCEPTED MANUSCRIPT
Journal of Applied Physics
AIP Publishing
This is the author's peer reviewed, accepted manuscript. However, the online version of record will be different from this version once it has been copyedited and typeset.
PLEASE CITE THIS ARTICLE AS DOI: 10.1063/5.0102206

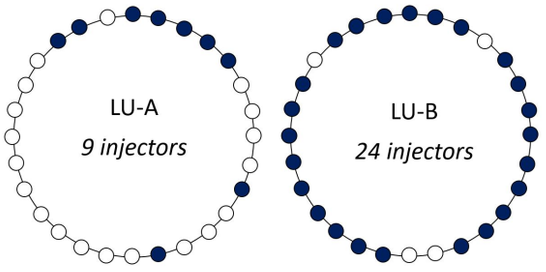

FIG. 1: Emitter distribution for both laboratory units, LU-A (left) and LU-B (right), during measurements.

B. Ion source: *ENPULSION NANO* laboratory unit

The *ENPULSION NANO* is engineered and produced by the Austrian company *Enpulsion GmbH*[19,20]. The thruster working principle is based on FEEP technology[21–23] and has been studied over 20 years by *FOTEC GmbH*[4,24–27]. The thruster uses indium, a molten metal, as propellant. The latter is used to wet[28] a porous emitter crown constituted of 28 sharp needles, also called injectors. To provide enough potential difference to form Taylor cones at the tip of each injectors[29,30] and start the ionization process a counter electrode termed extractor (V_{ex}) is placed around the emitter. The resulting local field strength at the apex of the Taylor cone ($\sim 10^9$ V/m) has twofold purpose i) it leads to particle extraction and ionization and ii) it accelerates the ions.

Results obtained in this work rely on measurements and analysis of the ion beam produced by two laboratory units (LU) version of this thruster. The lab units are not equipped with neutralisers considering the low current densities at stakes but also to ease current trace understanding. Emission current (I_{em}) and voltage (V_{em}) are controlled with a power processing unit (PPU) which allows accurate recordings with 1% reading accuracy. Due to experimental and time constraints the LUs had different injector distribution as showed in figure 1. This difference brings information on the influence of the firing conditions and ion beam velocity vector upon the ion-induced electron yield measured as described in section IV B. LU-A was used to asses the evolution of SEE yield with different foam material pore sizes, see section IV A. LU-B was used for the rest of the study. The thruster LU-A was fired at 1 mA while LU-B was fired at 1, 2, 3 and 4 mA. For each emission current different V_{em} are applied to vary the ion energy. Ions in the beam produced by the ENPULSION NANO are singly-charged. Without energy losses the ion energy reads $E_i = eV_{em}$[31].

III. METHOD

A. Ion current and collection efficiency

The ion current density angular distribution is obtained from the ratio between the ion current, averaged over 10 consecutive measurements at each angular position, and the collection area. The ion current I_{int} can be retrieved from the integration of the current measured on a plane which contains the thruster axis, e.g. following the angle θ from $-\pi/2$ to $\pi/2$ (sections IV D). We use the hypothesis of cylindrical symmetry around the thruster axis[13,17,32]. However, this assumption holds only if the amount of firing needles is sufficient and well distributed (e.g. LU-B). Therefore, $I_{i_{int}}$ reads:

$$I_{i_{int}} = \pi R^2 \int_{\frac{-\pi}{2}}^{\frac{\pi}{2}} j_i(\theta) \mid \sin(\theta) \mid d\theta, \tag{1}$$

with R being the distance from the probe inlet to the ion source emission plane, j_i the current density (A/m^2) and θ the angle between the probe centre axis and the ion source firing axis. Consequently, the ion collection efficiency reads[17,18]:

$$\eta_p = \frac{I_{i_{int}}}{I_{em}}. \tag{2}$$

Where I_{em} is the ion current emitted by the ion source and controlled by a power processing unit. Uncertainties are computed following equation 3 where σ is the standard deviation and u the corresponding uncertainty.

$$u = \frac{\sigma}{\sqrt{n}}, \tag{3}$$

with n the number of samples. The sum of each uncertainties is computed following a linear error propagation with 95% confidence (k=2) level which reads:

$$u = \sqrt{\sum_{i=1}^{n} u_i^2},\ u_{95\%} = 2u. \tag{4}$$

Previous studies[17,18] showed that with the right architecture a FC can accurately measure the ion current giving a value close to the one emitted by the thruster with $\pm 3\%$ with 95% confidence. During ion current measurement I_{em} and V_{em} are controlled and recorded by the thruster laboratory unit onboard telemetry. In the case of ion current density angular distribution set, thruster firing conditions are constantly monitored. Then, an average of 800 data samples acquired over 25 minutes with accuracy of 0.01%, negligible compared to the telemetry reading accuracy ($\sim$1%), gives the mean firing parameters.

B. Ion-induced electron emission yield (γ_{SEE})

Ion-induced electron emission (SEE) is known to be the cause of an artificial current rise when measuring ion current.

ACCEPTED MANUSCRIPT
Journal of Applied Physics
AIP Publishing
This is the author's peer reviewed, accepted manuscript. However, the online version of record will be different from this version once it has been copyedited and typeset.
PLEASE CITE THIS ARTICLE AS DOI: 10.1063/5.0102206

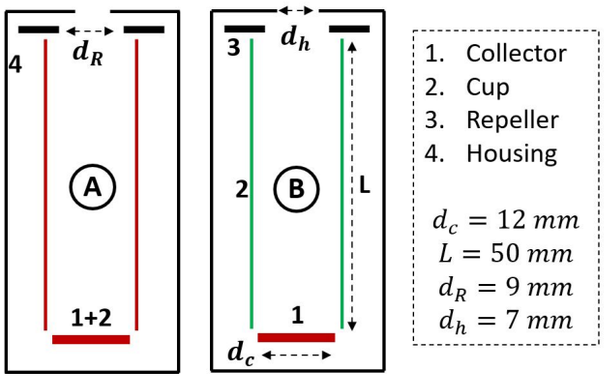

FIG. 2: Schematic of probe configuration used to measure γ_{SEE}

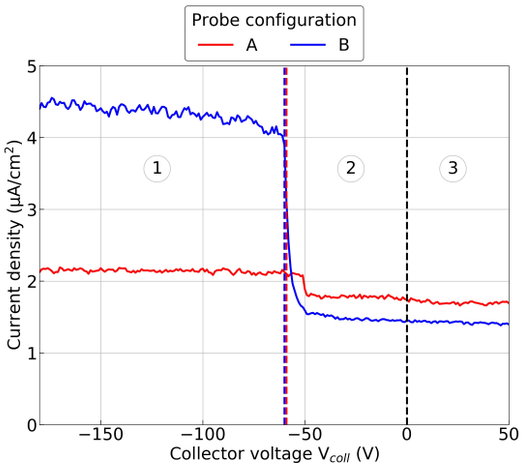

FIG. 3: I-V curves measured with different probe configurations. Probe A uses the collector and the cup as one electrode while with configuration B these two elements are electrically uncoupled. The two coloured dashed lines corresponds to V_{rep} (configuration A) or V_{cup} (configuration B) at -60 V. The black dashed line ease the visualisation for the transition from negative to positive voltages.

Therefore, it is fundamental to either properly recollect ion-induced electrons (SE) or to determine the rate of emitted SE to correct output consequently. The yield of SEE, γ_{SEE}, depends on projectile ion energy, incidence angle and collector material properties. Commonly, γ_{SEE} is determined by applying a voltage sweep on an ion collector V_{coll} placed downstream an electrode V_{ele} with a fixed negative voltage[33,34]. When $V_{coll} < V_{ele}$, the current measured on the collector is $I_c = I_{SEE}$, with I_{SEE} the ion current including the contribution from SEE. Then, when $V_{coll} > V_{ele}$, the current measured on the collector corresponds to the real ion current, $I_c = I_i$. Therefore, γ_{SEE} reads[35]:

$$\gamma_{SEE} = \frac{I_{SEE} - I_i}{I_i}. \tag{5}$$

However, if one uses the above mentioned probe architecture, and make the hypothesis that the whole ion flux is only collected by the probe rear part, two problems arise when $V_{coll} > V_{ele}$: 1) the collector will start to collect SE emitted by the electrode placed upstream, 2) a part of the ion current will be collected by the electrode and not the collector. Both case will induce a wrong estimation of SE yield. In our study we modified the architecture of a FC to get around this artificial yield rise, see figure 2. There, V_{ele} either refers to V_{rep} or V_{cup} depending on the probe configuration, A vs B. When configuration A is used the ion collector is the "cup + rear disk". For configuration B the ion collector is only the "rear disk". In both cases the electrode placed upstream right behind the probe aperture, termed repeller (V_{rep}),[17,32] is biased negatively to screen thermal electrons and ion-induced electrons due to plasma-probe interaction. Two IV curves, for an ion collector made of aluminium, are displayed in figure 3. They illustrate the problem stated above. Ion current is plotted as positive values. The ion current without SE contribution should correspond to the current measured in zone 2[18]. However, in this zone the two configurations A and B give different values with $I_B < I_A$. Figure 4 provides explanations for current measured in zone 1 and 2 for configuration A and B. In zone 1, SE are not recollected with both configurations, since V_{coll} is lower than the other one, hence an overestimated current. The current measured by B is increased due to SE from the ion collector located at the rear of the probe. The current measured by A is solely perturbs by ion-induced electrons that escape the cup which is characterized by the yield $\gamma_{L_{SEE}}$[18]. Therefore, in both cases the current is artificially increased but not with the same factor. Configuration A manages to recollect an important part of ion-induced electrons in zone 1. In zone 2, all ion-induced electrons are recollected as $V_{coll} > V_{ele}$, V_{ele} being V_{rep} and V_{cup} with configuration A and B, respectively. However, in B an additional parameter contributes to the current measured. The source cannot be properly characterized with the current experiment but is expected to be either due to 1) ions being now collected by the cup walls instead if the collector due to the electrode potential change or 2) ion induced electrons from the cup walls being now attracted by the collector due to the potential change. Figure 5 and 6 show the current change with the voltage inside probes A and B with a 60 conical collector made of aluminium 2017A. In configuration A (figure 5), the repeller is biased to -60 V and SE are recollected when V_{coll} overtakes V_{rep}. The shift observed is caused by a potential dip at the repeller aperture centre. While a current drop is observed on the collector (top), no specific change is seen on the repeller (bottom) at the same voltage. Therefore, it indicates that in zone 1 SE from the cup are not collected by the repeller, electrons leave the probe instead. Moreover the ion current measured in zone 2 by the repeller is 100 times lower than the collector current and therefore, can be neglected. A detailed description of ion current behaviour with A can be found elsewhere[17,18]. In configuration B (figure 6), a different behaviour is observed. The figure is divided into three plots. The first one (top) show current measured by the collector. The second plot (middle) displays the current acquired by the cup. The third one (bottom) compare the

ACCEPTED MANUSCRIPT
This is the author's peer reviewed, accepted manuscript. However, the online version of record will be different from this version once it has been copyedited and typeset.
PLEASE CITE THIS ARTICLE AS DOI: 10.1063/5.0102206

Journal of Applied Physics
AIP Publishing

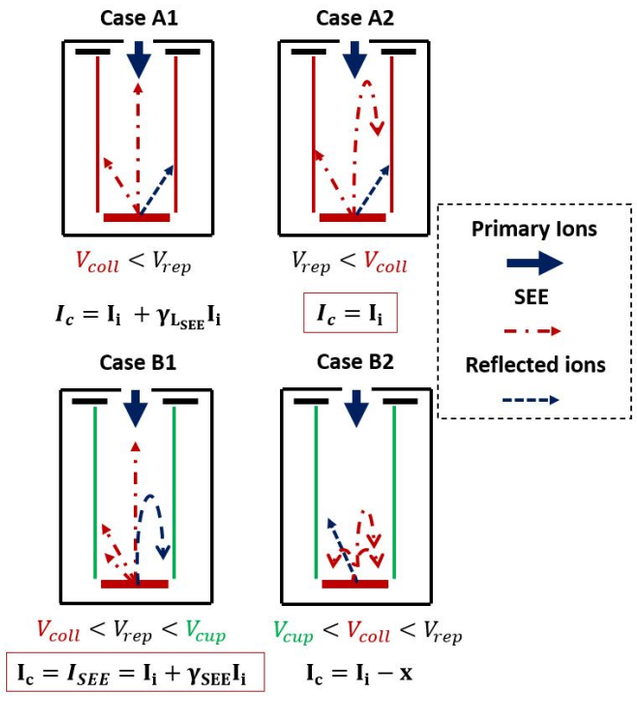

FIG. 4: Explanation of the measurement method to obtain γ_{SEE}

current measured with configuration A against the sum of currents acquired by the collector and cup with B. On the top and middle plot, three different voltages are applied to the cup: -60 V, 0 V and 20 V. In each cases the current value is the same on the collector and cup before and after SE recollection by the collector. Indeed in zone 1, the current measured on the cup is mainly from electrons, hence negative, corresponding to SE emitted by the collector. When V_{coll} overtakes V_{cup} the cup current becomes positive. The latter is larger than the current observed on the collector which decreases. When the voltage applied to the collector reaches 100 V near 90% of the ion current inside the probe is measured by the cup with only 10% remaining on the collector. In this configuration, SE from the collector are properly recollected by the latter but an additional electron current is collected as well and a large ion loss towards the cup sides is observed. On the third plot (bottom) we clearly see that the sum of currents measured on the cup and collector matches the current measured by FC A. The current maximum observed corresponds to the SE recollection at -60 V, corresponding to V_{ele}. Therefore, currents obtained with the FC $B1$ and FC $A2$ will be used in equation 5 to accurately determine γ_{SEE}. To measure I_i the probe voltages are fixed at $V_{coll} = -30V$ and $V_{rep} = -60V$. To acquire I_{SEE} we use $V_{coll} = -30V$ and $V_{rep} = 20V$. In this study γ_{SEE} is given for flat and conical aluminium 2017A collector, flat tungsten collector, stainless steel 316L as well as molybdenum and aluminium $AlSi7Mg$ foam with different pore sizes as described in table I.

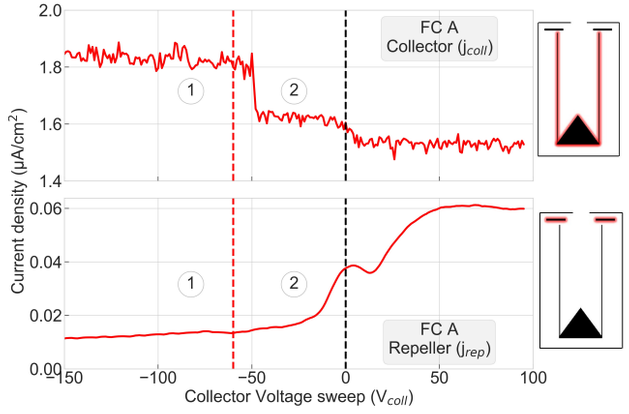

FIG. 5: Current measured on the collector + cup (top) and repeller (bottom) simultaneously during a voltage sweep on the collector. The probe is FC A with a 60 conical aluminium collector. The thruster fires at 2 mA and 6 kV.

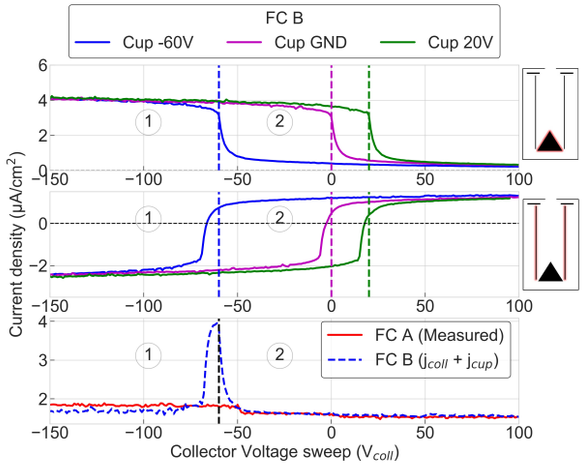

FIG. 6: Current acquired simultaneously on the collector (top) and cup (middle) during a voltage sweep on the collector. The probe is FC B with a 60 conical aluminium collector. The thruster fires at 2 mA and 6 kV. The bottom plot compares current acquired with FC A and FC B.

TABLE I: Details summary of each materials assessed as ion collector.

Material	Geometry	Properties	Name
Aluminum 2017A	conical	Plain, α_1 = 105	Alc
Aluminum 2017A	conical	Plain, α_2 = 60	Alc2
Aluminum 2017A	flat	Plain	Al
Aluminum 2017A	flat	Foam #1[36]	F1
Aluminum 2017A	flat	Foam #3[36]	F3
Aluminum 2017A	flat	Foam #6[36]	F6
Molybdenum	flat	Plain	Mo
Tungsten	flat	Plain	W
Stainless steel 316L	flat	Plain	S

ACCEPTED MANUSCRIPT
Journal of Applied Physics
AIP Publishing
This is the author's peer reviewed, accepted manuscript. However, the online version of record will be different from this version once it has been copyedited and typeset.
PLEASE CITE THIS ARTICLE AS DOI: 10.1063/5.0102206

IV. RESULTS AND DISCUSSION

A. γ_{SEE} for different materials

Figure 7 displays SEE yield measured following the method explained in section III B. The yields are plotted as a function of the mean indium ion energy for flat aluminium 2017A (a), tungsten (b), molybdenum (c) and stainless steel 316L (d) collector. These materials were chosen as they are widely used among the EP community as collector for electrostatic probes. Data is displayed for different ion current emission ranging from 1 to 4 mA. The extractor voltage is also displayed to assure similar conditions between measurements. One should note that yields are not given for every emission current at a given ion energy. This is due to the limit of the on-board power processing unit used for this experiment (i.e., total discharge, input power). It has been proved[35,37,38] that SEE yield can result from a combination of potential (PE) and kinetic (KE) electron emission. The two mechanisms rely on different energy transfer principles. PE emission results from electron excitation due to conversion of internal energy while KE emission occurs in the presence of kinetic energy transfer during collisions. The main difference is that PE is independent of the incoming ion energy and is driven by the collector material work function (ϕ) while KE strongly depends on the ion energy. In this study $E_i \gg \phi$, as ϕ is of the order of a few eV[35] for studied materials. Therefore, PE mechanism can be neglected and we consider KE to be the only phenomenon responsible for electron emission. Figure 7 shows that SEE yield increases monotonically for all material. However, while the yield is of the same order for molybdenum, tungsten and steel 316L, γ_{SEE} obtained with aluminium 2017A is 3.5 to 4.5 larger. Moreover, between the lowest and highest mean ion energy the growth rate differs for the four materials. Indeed, the rise is around 57% for molybdenum, 67% for tungsten, 72% for aluminium 2017A and approaches 95% for steel 316L. We note a deviation of the yield at 2mA for the aluminium collector even after several additional measurements. This behaviour is not yet explained. However, section IV B gives information on how the firing conditions (needles distribution, incidence angle of the ion influence) can easily modify the yield measured. Besides, some collector materials are more influenced than others.

It is interesting to compare how the evolution of γ_{SEE} for indium ions to yields induced by primary electron influences available in the literature. Both depend on the material surface quality (roughness, chemical composition) and the angle of incident[39] (see section IV C). However, we note that the secondary electron yield induced by ions increases with the ion energy whereas for primary electrons the yield increases until it reaches a maximum before decreasing[39,40]. Shih et al.[39] showed that secondary electron emitted by a surface greatly depends on the penetration depth (in microns) of the incoming primary particle. If P (the penetration-depth) is less than E (the escape-depth) the number of secondary electrons generated and then emitted increase with the primary energy. However, when P becomes larger than E, the escape rate of internal secondary electrons decreases quicker than the generation rate of the latter. Therefore, the yield decreases for higher primary energies. The maximum is reached when P is near E, which gives a bell-shape profile to the secondary primary electron curve. It is understood[41,42] that electrons have a penetration depth around 10 times larger than ions for a given energy. Consequently, the threshold value to see the decline of the yield with an increase of the energy for ions is at higher level than for primary electrons, hence not visible at the current energy studied.

B. Solid vs foam metal

Figure 8 shows γ_{SEE} obtained with different ion collector aluminium properties and geometries. Figure 8a presents the evolution of the yield for aluminium foams *AlSi7Mg* characterized by different pore diameters. F1 refers to pore size ranging from 0.2 to 0.35 mm and F6 has pore sizes from 0.63 to 3 mm. Note that the porosity remains 55%-65% for all foams. Here, the thruster is LU-A and fires at 1 mA. The yield increases monotonically for all foams. However, the yield is smaller for F6. In average γ_{SEE} drops by 26%±8.4% between F1 and F6. Nevertheless, the yield variation between low and high mean ion energy approaches 40%±3% for both collectors. The observed yield reduction can be caused by different SE emission sites. When increasing the pore size, SE originates from deeper locations inside the collector. Hence the probability to recollect SE before they escape the foam structure increases. Figure 8b shows the evolution of the SEE yield for a flat bulk aluminium 2017A collector (Al) and the same foam aluminium collector used in figure 8a. Here, ions are ejected by LU-B. First, γ_{SEE} is near 60%±8.5% lower for foam. Second, the difference between both yields slightly increases with the ion energy indicating that a foam structure is less influenced by the increase of energy.

It is observed that γ_{SEE} for F6 measured with LU-A and LU-B is not the same. Figure 9 shows the variation of γ_{SEE} for molybdenum (bottom) and F6 (top) obtained with different ion sources. Note that it was not possible to reproduce the exact same operation points as LU-A needed more extraction voltage to provide similar emission parameters. The PPU internal limits prevented to reach emission voltage below 5 kV for LU-A and above 6 kV for LU-B at 1 mA. γ_{SEE} obtained for F6 with LU-A increased by 84% and 98% for 5 kV and 6 kV, respectively. On the contrary, there are no major change for the molybdenum collector as the variations are within the uncertainties of the measurement method. Note that for both materials the rate of change between the minimum and maximum yield is identical +40% and +58% for LU-A and LU-B, respectively. The increase of the measured yield for F6 could be caused by higher dependency to the ion incidence angle than molybdenum. Indeed, due to the needle distribution and the large extractor voltage used with LU-A the ions going through the probe might not hit the collector with a velocity vector identical to those from LU-B. Owing to its foam structure, the probability to have ions hitting its surface with an incidence angle different than 0 increases. The next section brings insights into the effect of the incidence angle upon

ACCEPTED MANUSCRIPT
Journal of Applied Physics
AIP Publishing
This is the author's peer reviewed, accepted manuscript. However, the online version of record will be different from this version once it has been copyedited and typeset.
PLEASE CITE THIS ARTICLE AS DOI: 10.1063/5.0102206

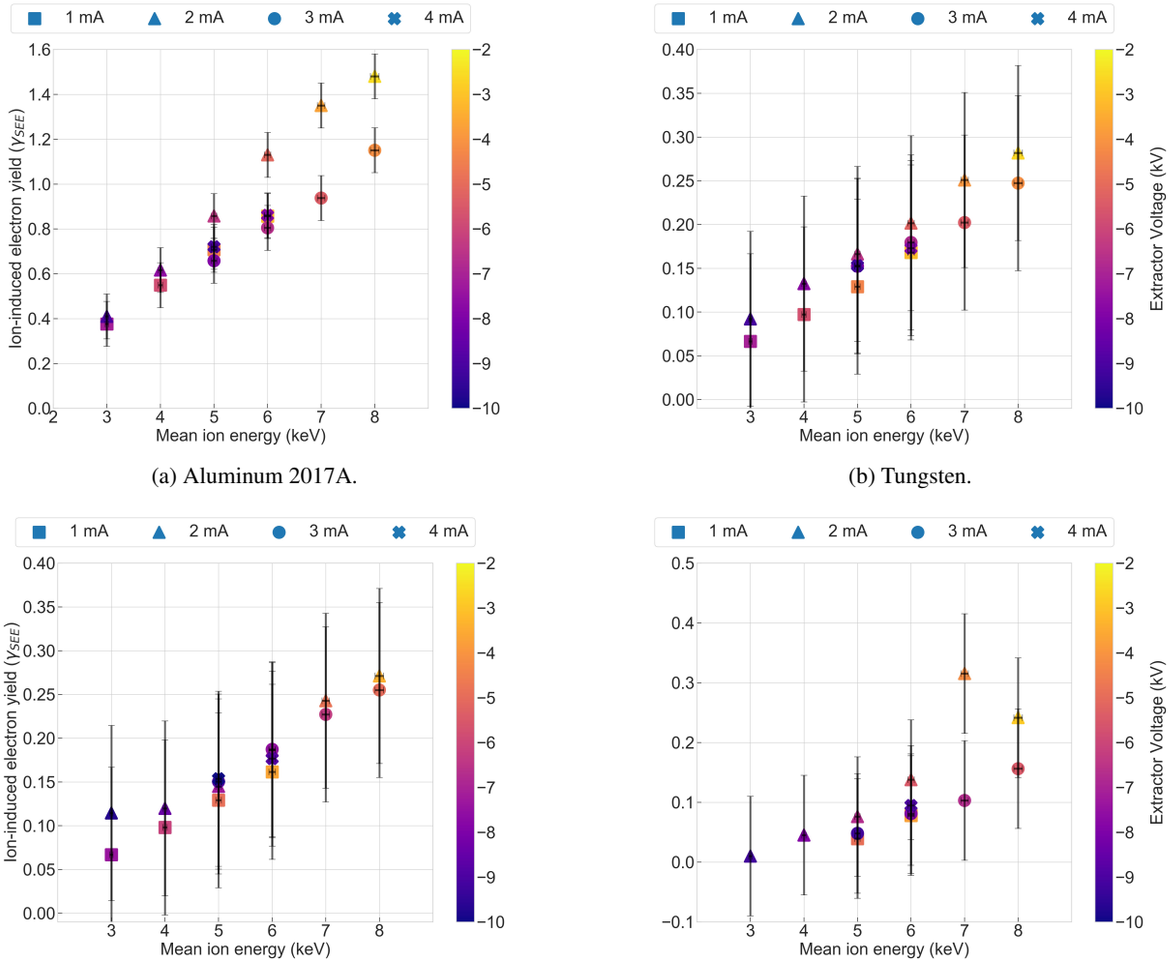

(a) Aluminum 2017A.

(b) Tungsten.

(c) Molybdenum.

(d) Stainless Steel 316L.

FIG. 7: Ion-induced electron yield (γ_{SEE}) from different flat ion collector obtained with the ion source LU-B firing with emission current set to 1, 2, 3 and 4 mA. The ion bombardment is supposed normal to the collector. (a) Aluminium 2017A, (b) Tungsten, (c) Molybdenum, (d) Stainless Steel 316L.

γ_{SEE}.

C. Collector geometry

Figure 10 shows the evolution of γ_{SEE} for different aluminium 2017A collector geometry with the ion source LU-B. Once more the yield increases monotonically with the bombarding mean ion energy. Here, we assume that ions entering the probe have a velocity vector purely perpendicular to the probe inlet plane. Therefore, when the angle which defines the conical shape of the collector decreases, the incidence angle (θ) increases. In this case, ions hit Alc with $\theta = 37.5$ and Alc2 with $\theta = 60$. We observe that increasing the incidence angle increases the yield of SEE. For higher θ it is easier for an ion to rip off electrons from the surface. In average, between Al (flat) and Alc the yield increases by 19.5%±3.4%. From Alc to Alc2 the yield increases by 14.3%±3% at the highest mean ion energy.

D. Ion-induced electron mitigation.

We have shown in the aforementioned sections that the ion current from an indium-based ion source acquired with an electrostatic probe depends significantly on the ion collector material properties and geometry. Nevertheless, all these perturbations can be counteract with the right probe architecture and voltage configuration, as showed in figure 11. Figure 11a shows the ion current density distribution acquired with a flat aluminium collector disturbed or not by ion-induced electron emission. The right plot of figure 11a displays the corresponding probe ion collection efficiency using equation 1 and 2. When the ion-induced electron effects are completely suppressed, the probe efficiency is the same no matter the thruster firing condition. Similarly, figure 11b shows that without SE

ACCEPTED MANUSCRIPT
Journal of Applied Physics
AIP Publishing
This is the author's peer reviewed, accepted manuscript. However, the online version of record will be different from this version once it has been copyedited and typeset.
PLEASE CITE THIS ARTICLE AS DOI: 10.1063/5.0102206

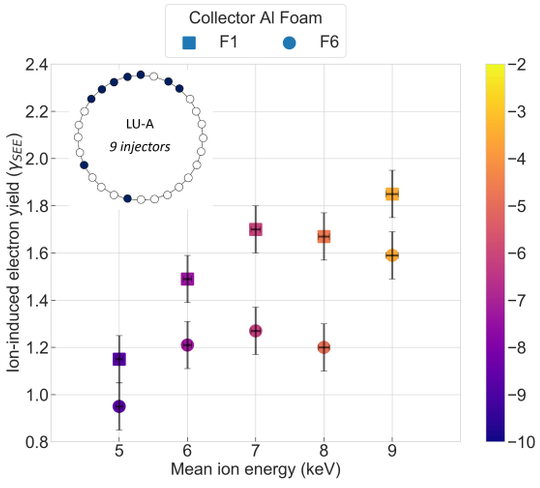

(a) γ_{SEE} obtained with the ion source LU-A for different aluminium *AlSi6Mg* foams F1 (square) and F6 (circle). The ion source is operated at 1 mA

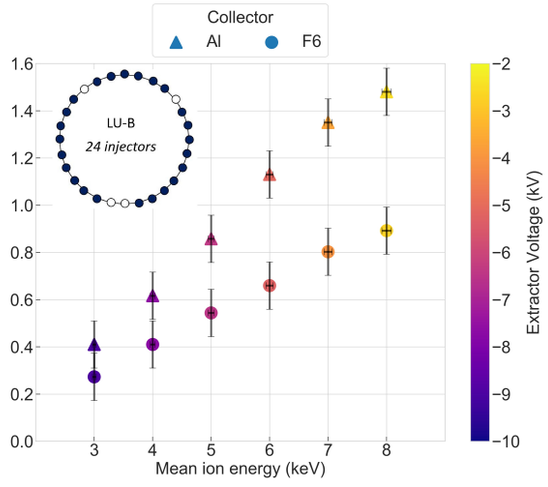

(b) γ_{SEE} obtained with the ion source LU-B for different aluminium collectors. Al (triangle) is flat bulk aluminium and F6 (circle) is foam aluminium *AlSi6Mg* (same as shown in figure 8a). The ion source is operated at 2 mA.

FIG. 8: Influence on computed γ_{SEE} of the ion collector material property. (a) γ_{SEE} for different aluminium *AlSi6Mg* foams. (b) γ_{SEE} for different aluminium collector types.

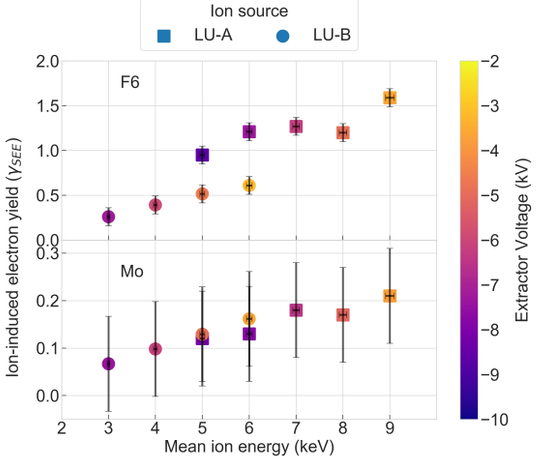

FIG. 9: γ_{SEE} variation for F6 and molybdenum (Mo) when measuring with LU-A (squares) and LU-B (circles).

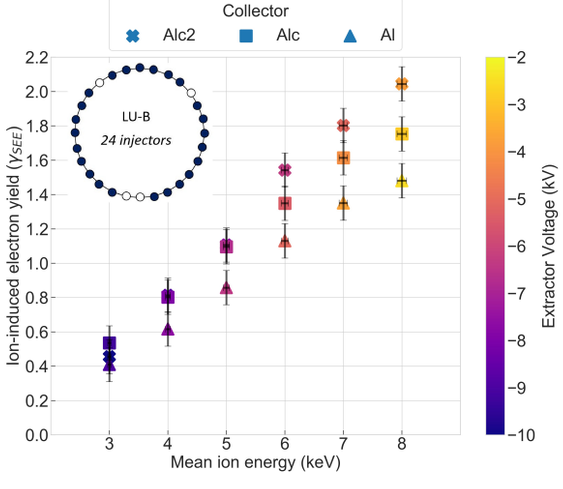

FIG. 10: Ion-induced electron yield obtained with the ion source LU-B for different collector geometries. LU-B emission current is set to 2 mA.

effects the ion current density distribution is independent of the collector material. The plots show clearly that the ion current density distribution acquired from a FEEP thruster strongly depends on ion-induced electron effects. Consequently, to retrieve ions information from the thruster plume a Faraday cup is warmly recommended as its architecture makes ion-induced electron emission perturbations simpler to mitigate, hence improving measurement reliability.

V. CONCLUSION

In this study, we have measured the ion-induced electron yield γ_{SEE} of different collector materials bombarded by keV-range energy indium ions. To enable such measurements a new probe design, based on a Faraday cup architecture, was developed. The collected ion flux is defined by the aperture of the probe casing front part. A negative voltage is applied to a repeller placed behind the casing aperture to prevent perturbations induced by plasma-probe interaction to reach the ion

ACCEPTED MANUSCRIPT
Journal of Applied Physics
AIP Publishing
This is the author's peer reviewed, accepted manuscript. However, the online version of record will be different from this version once it has been copyedited and typeset.
PLEASE CITE THIS ARTICLE AS DOI: 10.1063/5.0102206

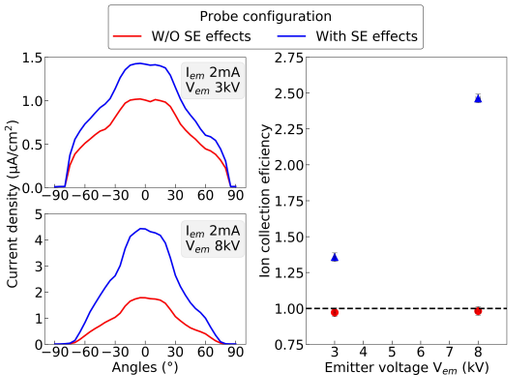

(a) Beam profiles (left) and related ion collection efficiency (right) acquired with a flat aluminium 2017A collector showing the effect of SE on ion current retrieval. The ion source fires at 2 mA with emitter potential set at 3 kV and 8 kV.

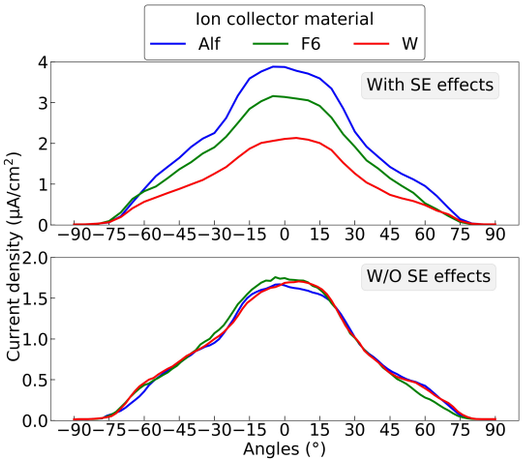

(b) Beam profile acquired with (top) and without (bottom) SE effects for different collector materials. Data was acquired for the ion source LU-B operating at 2 mA and 7 kV.

FIG. 11: Effects of ion-induced electron emission during ion current angular density distribution measurements for different ion source operation points (a) and different collector material (b).

collector. The latter has a cup-like shape (FC *A*). It can be divided into a simple cylinder and a disk (FC *B*) without modifying the experiment ambient conditions. From the currents acquired with FC *A* and FC *B*, with specific voltage variations, it was possible to estimate the SEE yield. It was shown that the yield varies linearly with the beam energy no matter the material. In the case of solid and flat materials such as tungsten and molybdenum, the SEE yield contributes to a variation from 10 to 30% of the measured current for low and high energy respectively. For solid and flat steel 316L collector, the yield does not exceed 10% for ion energy up to 5 keV and becomes negligible below 3 keV. For more energetic ions the SEE yield can contribute to rise the current by 30%. On the contrary, γ_{SEE} for flat aluminium 2017A collectors is significantly larger and can increase the measured current by 40 to 150%. In a second step, the structure of the material was studied. Aluminium foams with different pore sizes and constant porosity (55-60%) were used. We observed a diminution of the yield between the solid and the foam version. We also observed that changing the incidence angle between the collector and the ion trajectory affects the SEE yields. Nonetheless, the variation is less with low SEE yield materials like molybdenum. The lowest yield recorded for an aluminium 2017A collector was at 0 and the most important was for the largest incidence angle. Overall, we demonstrated that ion-induced electron is a major perturbation for ion current measurements with an electrostatic probe in the plume of a FEEP indium-based thruster. The yield depends largely on material and shape disturbances can be properly mitigated by the use a probe architecture similar to a Faraday cup. The probe design allows to greatly mitigate perturbations induced by SEE.

ACKNOWLEDGMENTS

V.Hugonnaud benefits from an ENPULSION PhD grant. Authors would like to thank Dr. Pr. Aumayr for his support on theoretical subject regarding plasma diagnostics design and behaviour. Additionally, we would like to thank C.Scharlemann, head of the FH Wiener Neustadt Aerospace department, for sharing their facilities.

[1] T.E.Sheridan, "How big is a small Langmuir probe," Physics of Plasmas **7** (2000), 10.1063/1.874162.
[2] V.I.Demidov, S.V.Ratynskaia, and K.Rypdal, "Electric probes for plasmas, the link between theory and instrument," Review of scientific instruments **73** (2002), 10.1063/1.1505099.
[3] S.Mazouffre and L.Grimaud, "Characteristics and Performances of a 100-W Hall Thruster for Microspacecraft," IEEE Transaction on plasma science **46**, 330–337 (2018).
[4] S.Keerl, W.Engel, N.S.Mühlich, J.Fries, and B.Seifert, "Two-dimensional plasma plume density characterisation of the IFM Nano Thruster," in *36th International Electric Propulsion Conference* (2019).
[5] C.M.Marerese, N.Majumdar, J.M.haas, G.Williams, L.B.King, and A.D.Gallimore, "Development of a single-orifice Retarding Potential Analyser for Hall Thruster Plume Characterization," in *25th International Electric Propulsion Conference* (1997).
[6] F.F.Chen, "Langmuir probe analysis for high density plasmas," Physics of Plasmas **8** (2001), 10.1063/1.1368874.
[7] R.L.Merlino, "Understanding Langmuir probe current-voltage characteristics," American Journal of Physics **75** (2007), 10.1119/1.2772282.
[8] K.J.Terhune and L. King, "Ion and Droplet Mass Measurement of an Electrospray Emitter using ExB filter," in *32nd International Electric Propulsion Conference* (2011).
[9] J.P.Sheehan and N.Hershkovitz, "Emissive probes," Plasma Sources Science and Technology **20**, 063001 (2011).
[10] N.Teshigahara, S.Shinohara, Y. Yamagata, D. Kuwahara, and M. Watanabe, "Development of 2D Laser-Induced Fluorescence (LIF) System in High-Density Helicon Plasma," Plasma and Fusion Research **9**, 3406055 (2014).
[11] B.S.Rawat, S.Vala, M.Abhangi, R.Kumar, and S.Chauhan, "Design and simulation of 10kW Faraday cup for ion beam current," in *25th International Conference on Nuclear Engineering ICONE25* (2017).

ACCEPTED MANUSCRIPT
Journal of Applied Physics
AIP Publishing
This is the author's peer reviewed, accepted manuscript. However, the online version of record will be different from this version once it has been copyedited and typeset.
PLEASE CITE THIS ARTICLE AS DOI: 10.1063/5.0102206

[12] S.Mazouffre, G.Largeau, L.Garrigues, C.Boniface, and K.Dannenmayer, "Evaluation of various probe designs for measuring the ion current density in a Hall thruster plume," in *35th International Electric Propulsion Conference* (2017).

[13] D.L.Brown, M.L.R.Walker, J.Szabo, W.Huang, and J.E.Foster, "Recommended Practice for Use of Faraday Probes in Electric Propulsion Testing," Journal of Propulsion and Power **33** (2017), 10.2514/1.B35696.

[14] D.Krejci, F. Mier-Hicks, R.Thomas, T.Haag, and P.Lozano, "Emission Characteristics of Passively Fed Electrospray Microthruster with Propellant Reservoirs," .

[15] B.Vincent, S.Tsikata, S.Mazouffre, T.Minea, and J.Fils, "A compact new incoherent Thompson scattering diagnostic for low-temperature plasma studies," Plasma Sources Sci. Technol. **27**, 055002 (2018).

[16] R.R.Hofer, M.L.R.Walker, and A.D.Gallimore, "A Comparison of Nude and Collimated Faraday Probes for Use with Hall Thrusters," in *27th International Electric Propulsion Conference* (2001).

[17] V.Hugonnaud, S.Mazouffre, D.Krejci, B.Seifert, and C.Scharlemann, "Faraday cup design for low power electric thrusters," in *Space Propulsion 2020+1* (2021).

[18] V.Hugonnaud, S.Mazouffre, and D.Krejci, "Faraday cup sizing for electric propulsion ion beam study: Case of a Field-Emission Electric Propulsion thruster," Review of Scientific Instrument **92**, 084502 (2021).

[19] D.Krejci and A.Reissner and T.Schoenherr and B.Seifert and Z.Saleem and R.Alejos, "Recent flight data from IFM Nano Thrusters in a low earth orbit," in *36th International Electric Propulsion Conference* (2019).

[20] T.Schoenherr and B.Little and D.Krejci and A.Reissner and B.Seifert, "Development, Production, and Testing of the IFM Nano FEEP Thruster," in *36th International Electric Propulsion Conference* (2019).

[21] S.Marcuccio, A.Genovese, and M.Andrenucci, "Experimental Performance of Field Emission Microthrusters," Journal of Propulsion and Power **14** (1998), 10.2514/2.5340.

[22] A. Genovese, W.Steiger, and M. Tajmar, "Indium FEEP microthruster: Experimental characterization in the 1-100μN range," in *37th AIAA/ASME/SAE/ASEE Joint Propulsion Conference and Exhibit* (2001).

[23] M.Tajmar, A.Genovese, and W.Steiger, "Experimental Performance of Field Emiision Microthrusters," Journal of Propulsion and Power **20** (2004), 10.2514/2.5340.

[24] I.Vasiljevich, M.Tajmar, W.Grienauer, F.Plesescu, N.Buldrini, J. D. Amo, B.Carnicero-Dominguez, and M.Betto, "Development of an Indium mN-FEEP Thruster," in *44th AIAA/ASME/SAE/ASEE Joint Propulsion Conference and Exhibit* (2008).

[25] D.Jelem, B.Seifert, R.Sypniewski, N.Buldrini, and A.Reissner, "Performance mapping and qualification of the IFM Nano thruster EM for in orbit demonstration," in *53rd AIAA/SAE/ASEE Joint Propulsion Conference* (2017).

[26] D.Jelem, A.Reissner, B.Seifert, N.Buldrini, L.Wilding, and D.Krejci, "Direct thrust and plume divergence measurements of the IFM Nano Thruster," Advances in Space Research **62**, 3398–3404 (2018).

[27] N.Mühlich, S.Keerl, W.Engel, E.Ceribas, and R-J.Koopmans, "Retarding Potential Analyser Development for Low Density FEEP Thruster Beam Diagnostics," in *36th International Electric Propulsion Conference* (2019).

[28] I.Vasiljevich, N.Buldrini, F.Plesescu, M.Tajmar, M.Betto, and J. D. Amo, "Porous Tungsten Crown Multiemitter Testing Programmes Using Three Different Grain Sizes and Sintering Procedures," in *The 32nd International Electric Propulsion Conference* (2011).

[29] G.I.Taylor, "Desintegration of water drops in an electric field," Royal Society **280** (1964), 10.1098/rspa.1964.0151.

[30] J. L. Mora and I. Loscertales, "The current emitted by highly conducting Taylor cones," Journal of Fluid Mechanics **260**, 155–184 (1994).

[31] N.S.Mühlich, B.Seifert, and F.Aumayr, "IFM Nano Thruster performance studied by experiments and numerical simulations," Journal of Physics D: Applied Physics **54**, 095203 (2020).

[32] V.Hugonnaud and S.Mazouffre, "Optimization of a Faraday cup collimator for electric propulsion device beam study: Case of a Hall thruster," Applied Sciences , 2419.

[33] C.Corbella, A.Marcak, T. de los Arcos, and A. von Keudell, "Revising secondary electron yields of ion-sputerred metal oxides," Journal of Physics D: Applied Physics **49** (2016), 10.1088/0022-3727/49/16/16LT01.

[34] L.Habl, D.Rafalskyi, and T.Lafleur, "Secondary electron emission due to multi-species iodine ion bombardment of different target materials," Journal of Applied Physics **129**, 153302 (2021).

[35] H. Eder, W. Messerschmidt, H. Winter, and F. Aumayra, "Electron emission from clean gold bombarded by slow Au^{q+} (q=1–3) ions," Journal of Applied Physics **87** (2000).

[36] Exxentis, "Exxentis Website Homepage,".

[37] R. A. Baragiola and P. Riccardi, "Critical potentials in secondary electorn emission from Iron, Nickel and Molybdenum," Reactive Sputter Deposition **109** (1965).

[38] E.V.Alonso, M.A.Alurralde, and R.A.Baragiola, "Kinetic electron emission from solids induced by slow heavy ions," Surface science **166**, 155–160 (1986).

[39] A.Shih, J.Yater, C.Hor, and R.Abrams, "Secondary electron emission studies," Applied Surface Science **111**, 251–258 (1997).

[40] V.Baglin, J.Bojko, O.Gröbner, B.Henrist, N.Hilleret, C.Scheuerlein, and M.Taborelli, "The secondary electron yield of technical materials and its variation with surface treatments," in *EPAC* (2000) pp. 217–221.

[41] J.R.Young, "Penetration of Electrons and Ions in Aluminum," Journal of Applied Physics **27** (1956), doi.org/10.1063/1.1722186.

[42] P.Li, S.Chen, H.Dai, Z.Yang, Z.Chen, Y.Wang, Y.Chen, W.Peng, W.Shana, and H.Duan, "Recent advances in focused ion beam nanofabrication for nanostructures and devices: fundamentals and applications," Journal of Applied Physics **13** (2020), 10.1039/D0NR07539F.

AIP Publishing
Journal of Applied Physics
ACCEPTED MANUSCRIPT

This is the author's peer reviewed, accepted manuscript. However, the online version of record will be different from this version once it has been copyedited and typeset.
PLEASE CITE THIS ARTICLE AS DOI: 10.1063/5.0102206

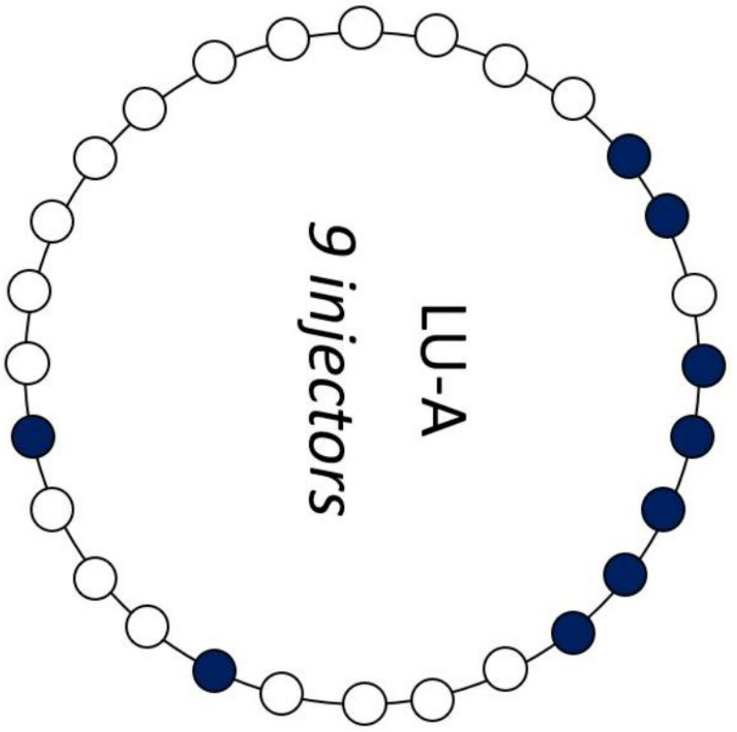

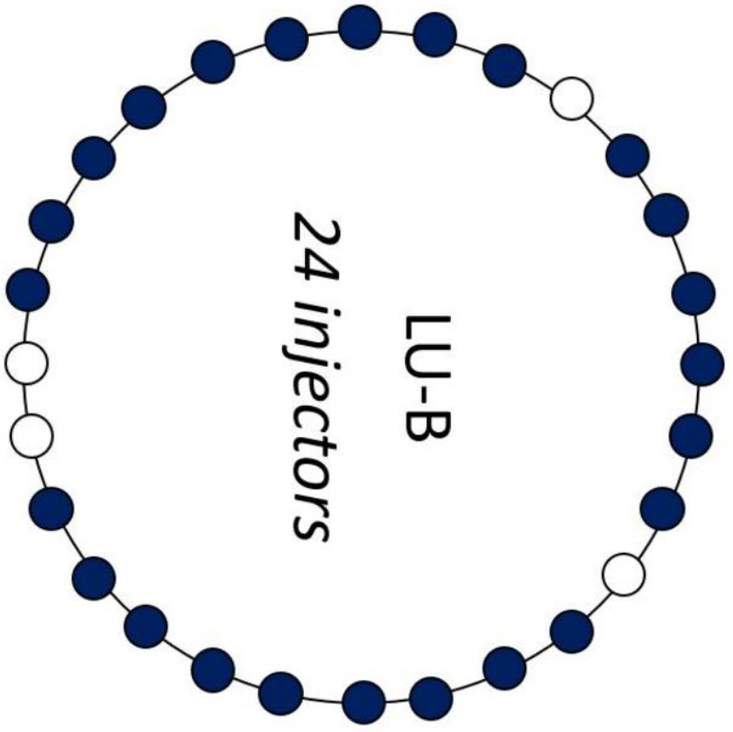

ACCEPTED MANUSCRIPT

This is the author's peer reviewed, accepted manuscript. However, the online version of record will be different from this version once it has been copyedited and typeset.
PLEASE CITE THIS ARTICLE AS DOI: 10.1063/5.0102206

Journal of Applied Physics

AIP Publishing

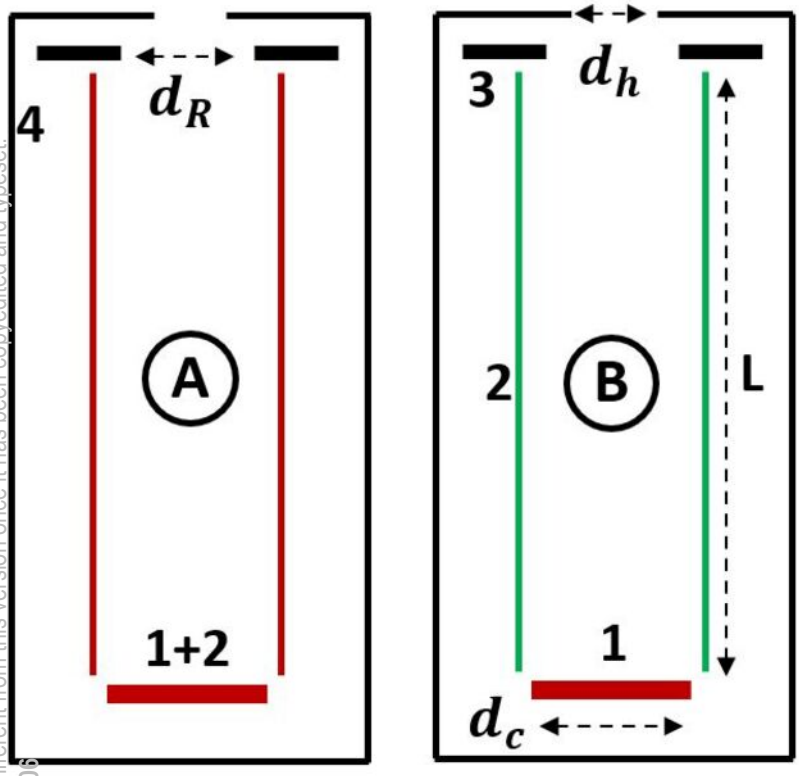

1. Collector
2. Cup
3. Repeller
4. Housing

$d_c = 12\ mm$
$L = 50\ mm$
$d_R = 9\ mm$
$d_h = 7\ mm$

ACCEPTED MANUSCRIPT

Journal of Applied Physics

AIP Publishing

This is the author's peer reviewed, accepted manuscript. However, the online version of record will be different from this version once it has been copyedited and typeset.
PLEASE CITE THIS ARTICLE AS DOI: 10.1063/5.0102246

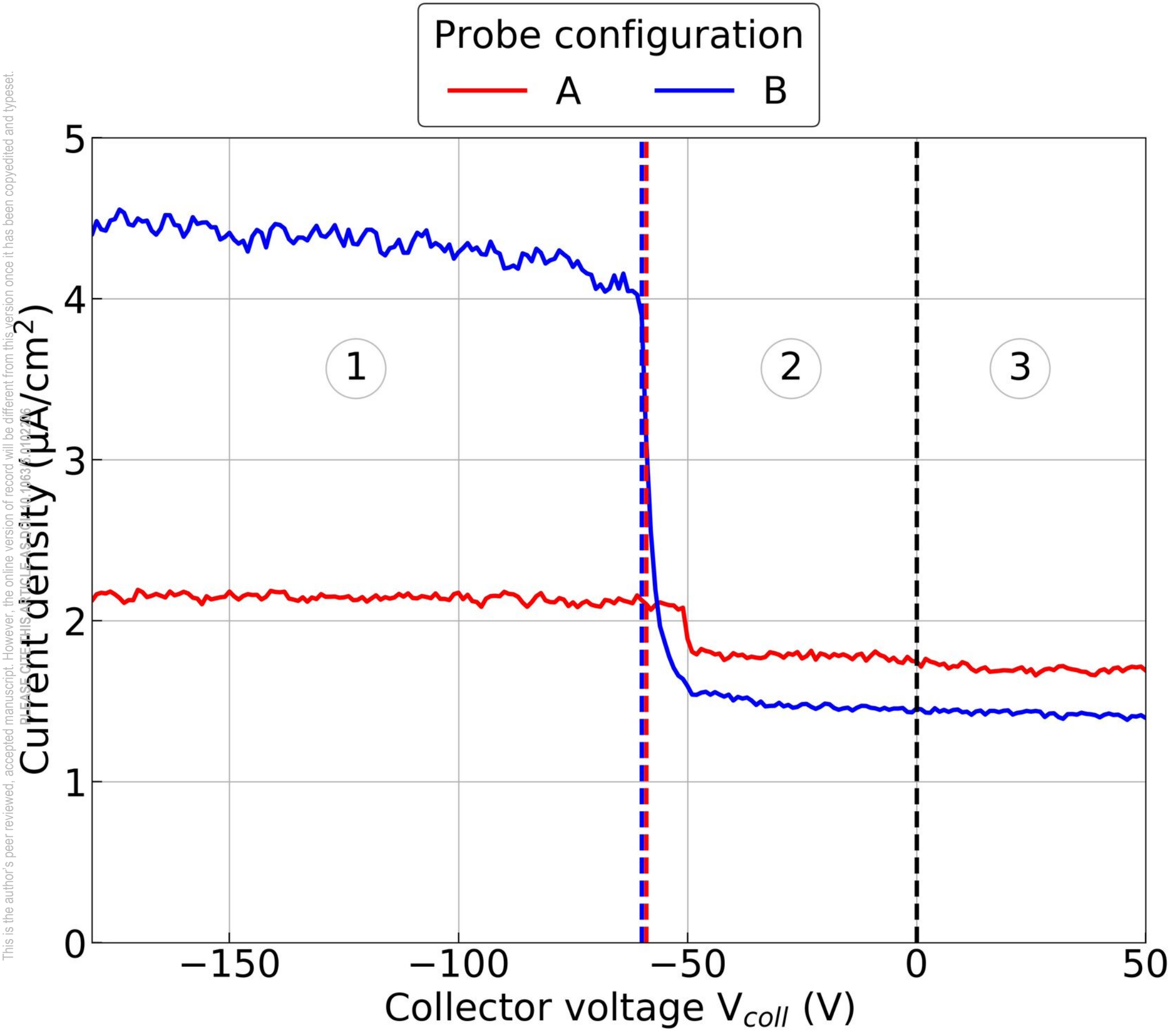

ACCEPTED MANUSCRIPT

Journal of Applied Physics

AIP Publishing

This is the author's peer reviewed, accepted manuscript. However, the online version of record will be different from this version once it has been copyedited and typeset.
PLEASE CITE THIS ARTICLE AS DOI: 10.1063/5.0102206

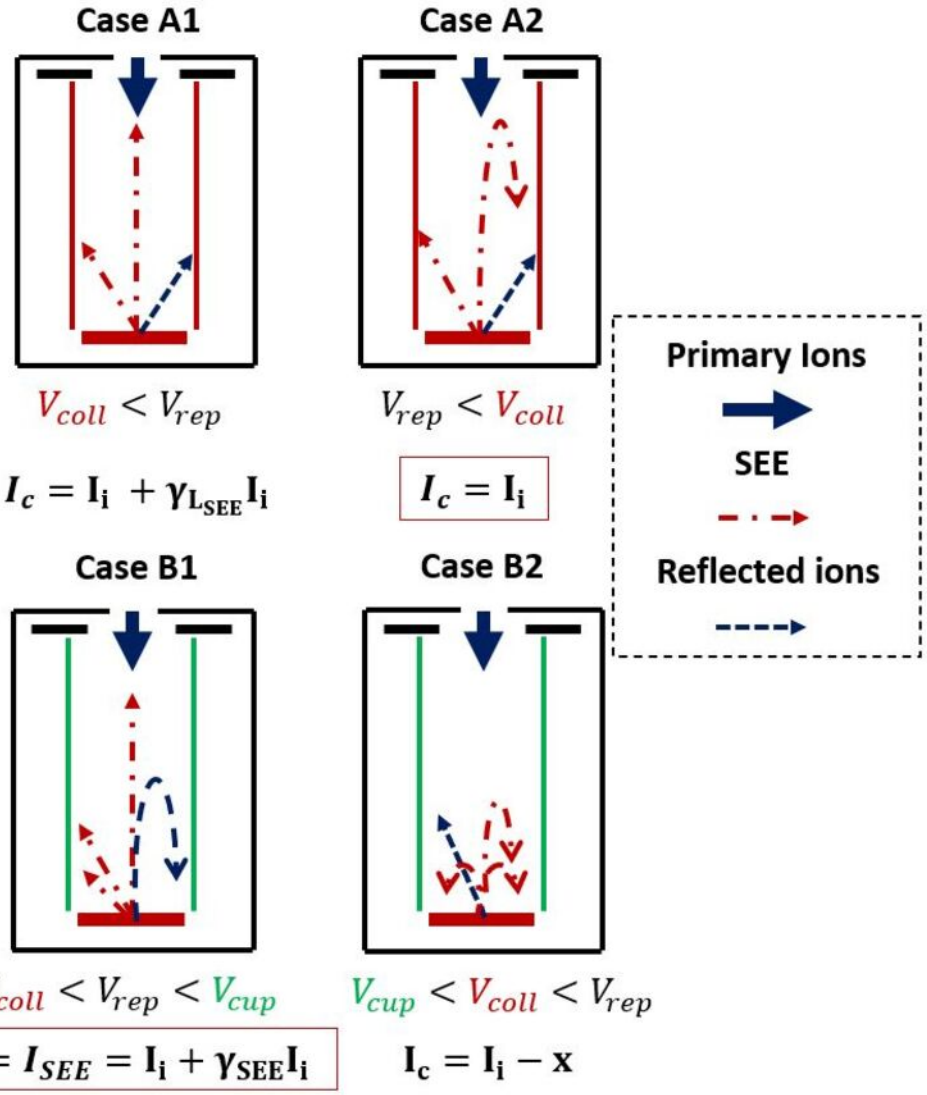

ACCEPTED MANUSCRIPT

This is the author's peer reviewed, accepted manuscript. However, the online version of record will be different from this version once it has been copyedited and typeset.
PLEASE CITE THIS ARTICLE AS DOI: 10.1063/5.0402306

Journal of Applied Physics

AIP Publishing

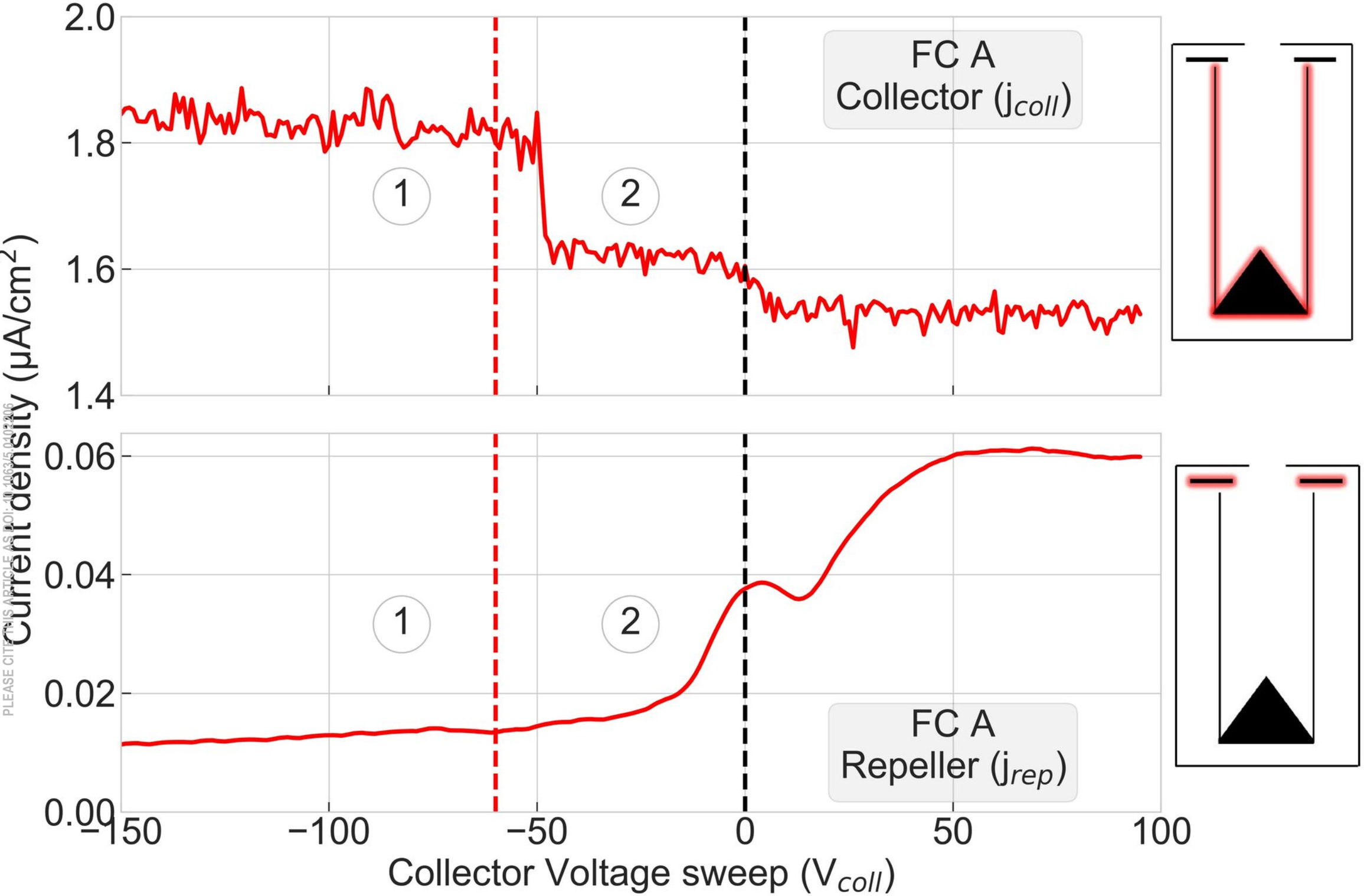

ACCEPTED MANUSCRIPT

Journal of Applied Physics

AIP Publishing

This is the author's peer reviewed, accepted manuscript. However, the online version of record will be different from this version once it has been copyedited and typeset.
PLEASE CITE THIS ARTICLE AS DOI: 10.1063/5.0102276

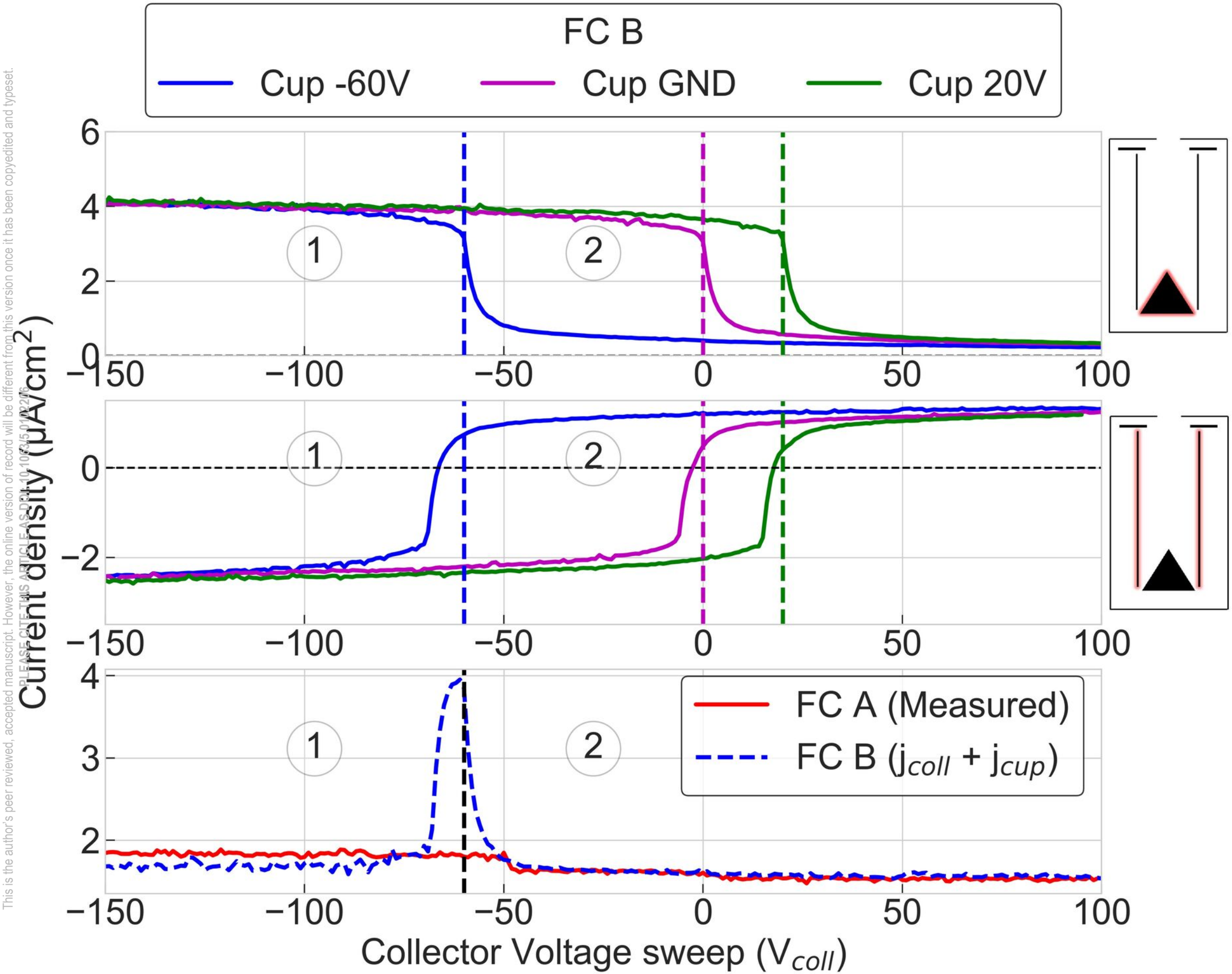

ACCEPTED MANUSCRIPT
Journal of Applied Physics
AIP Publishing
This is the author's peer reviewed, accepted manuscript. However, the online version of record will be different from this version once it has been copyedited and typeset.
PLEASE CITE THIS ARTICLE AS DOI: 10.1063/5.0102206

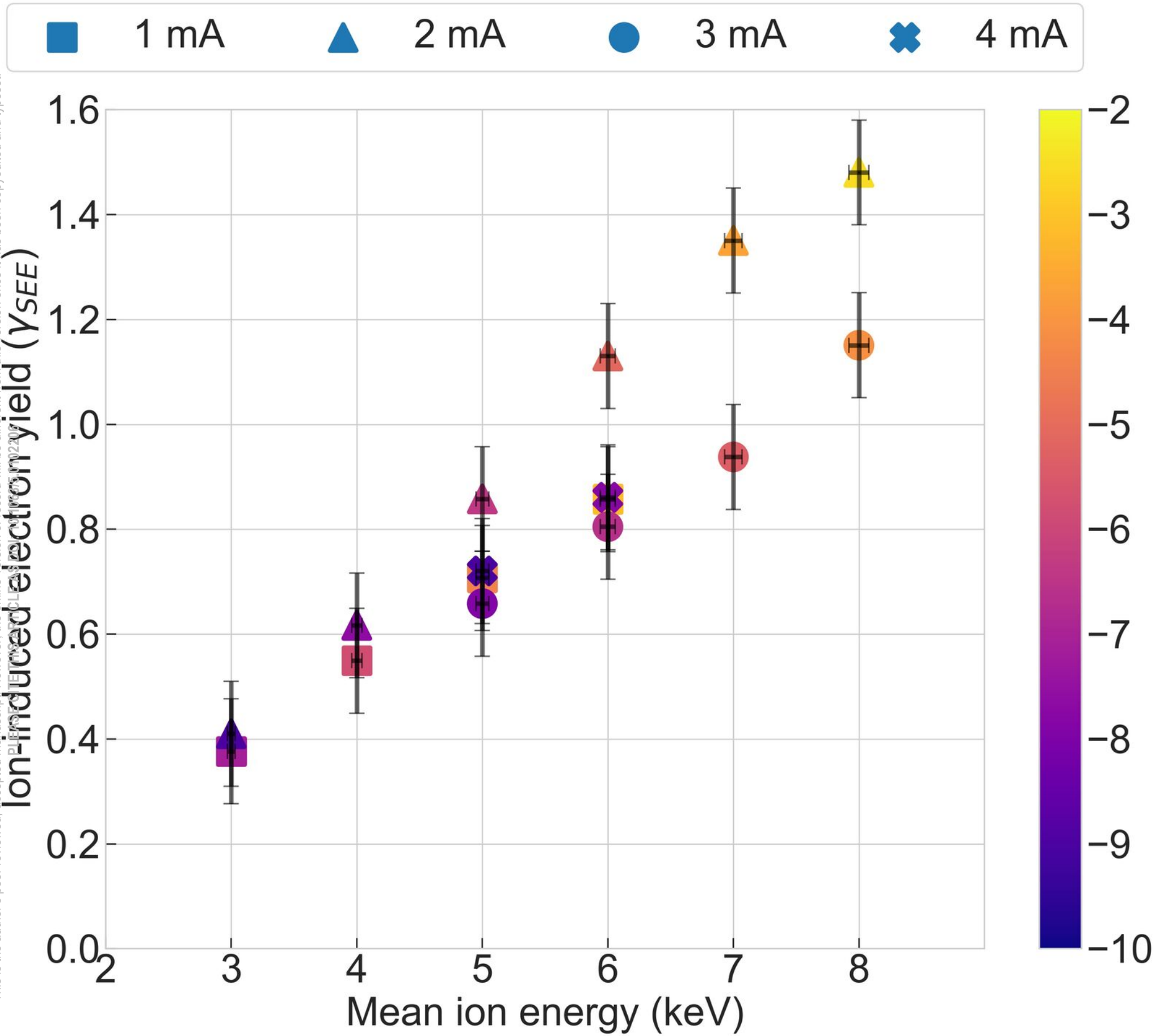

ACCEPTED MANUSCRIPT

Journal of Applied Physics

AIP Publishing

This is the author's peer reviewed, accepted manuscript. However, the online version of record will be different from this version once it has been copyedited and typeset.
PLEASE CITE THIS ARTICLE AS DOI: 10.1063/5.0102206

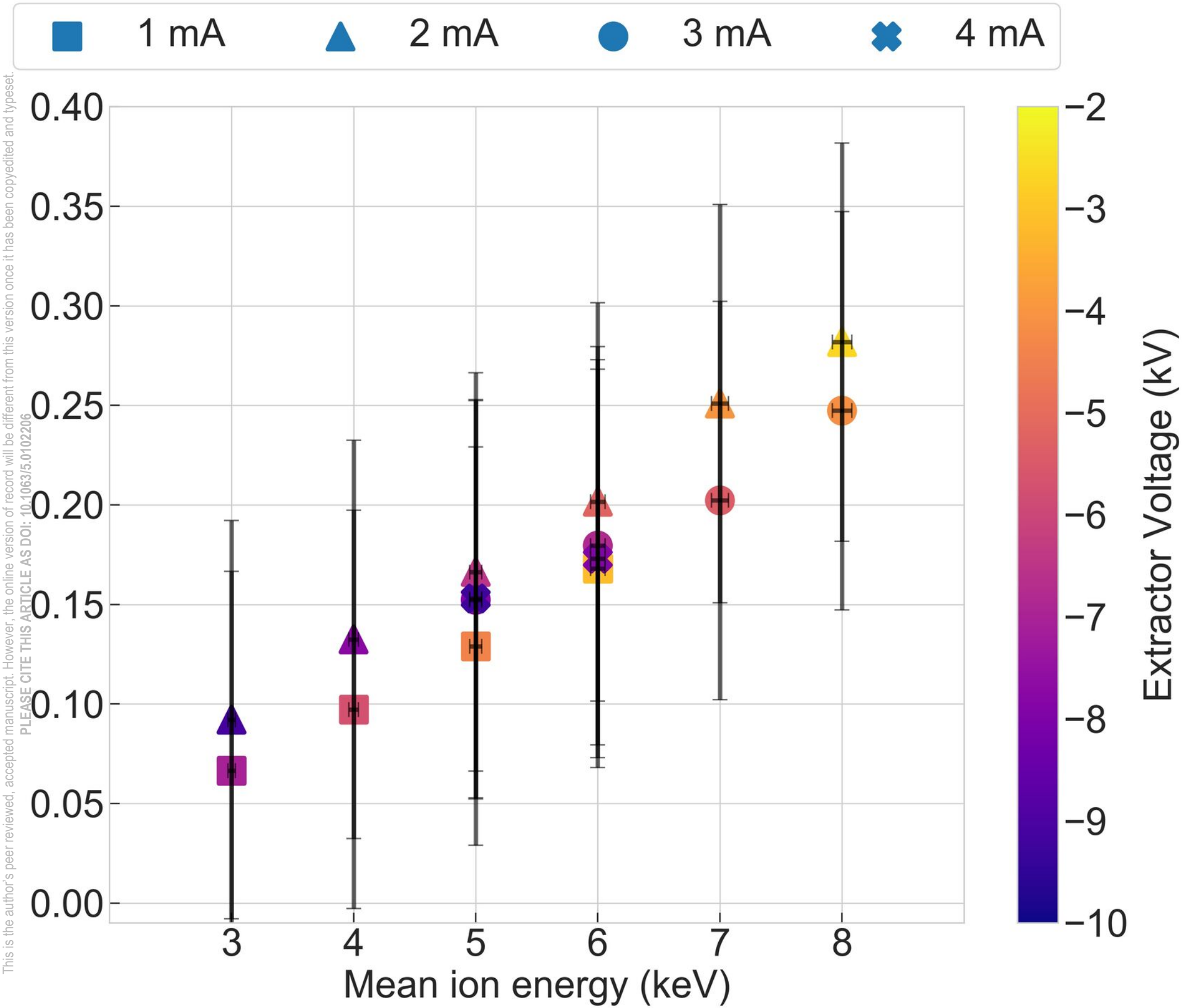

ACCEPTED MANUSCRIPT
Journal of Applied Physics
AIP Publishing
This is the author's peer reviewed, accepted manuscript. However, the online version of record will be different from this version once it has been copyedited and typeset.
PLEASE CITE THIS ARTICLE AS DOI: 10.1063/5.0102206

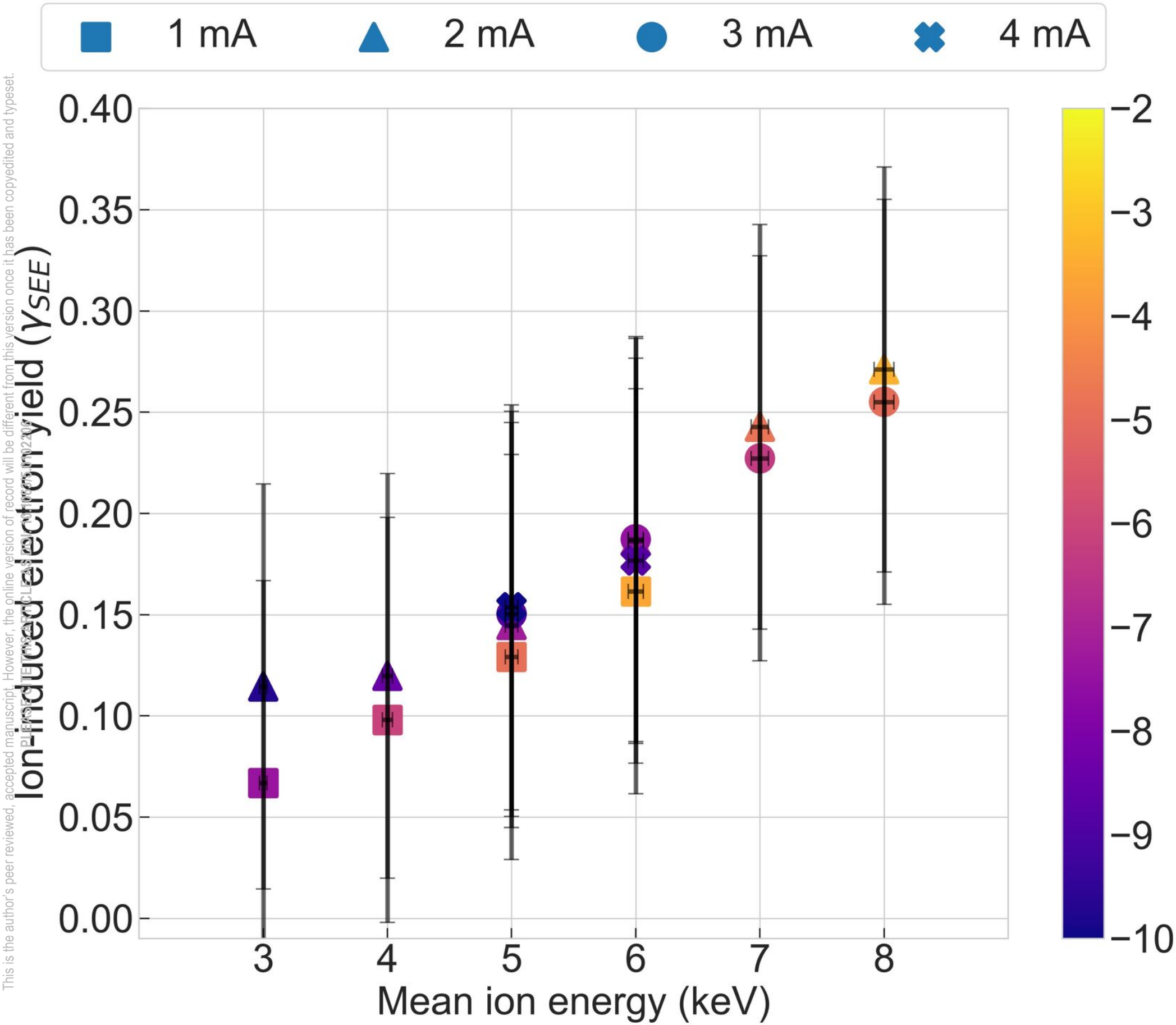

ACCEPTED MANUSCRIPT

Journal of Applied Physics

AIP Publishing

This is the author's peer reviewed, accepted manuscript. However, the online version of record will be different from this version once it has been copyedited and typeset.
PLEASE CITE THIS ARTICLE AS DOI: 10.1063/5.0102206

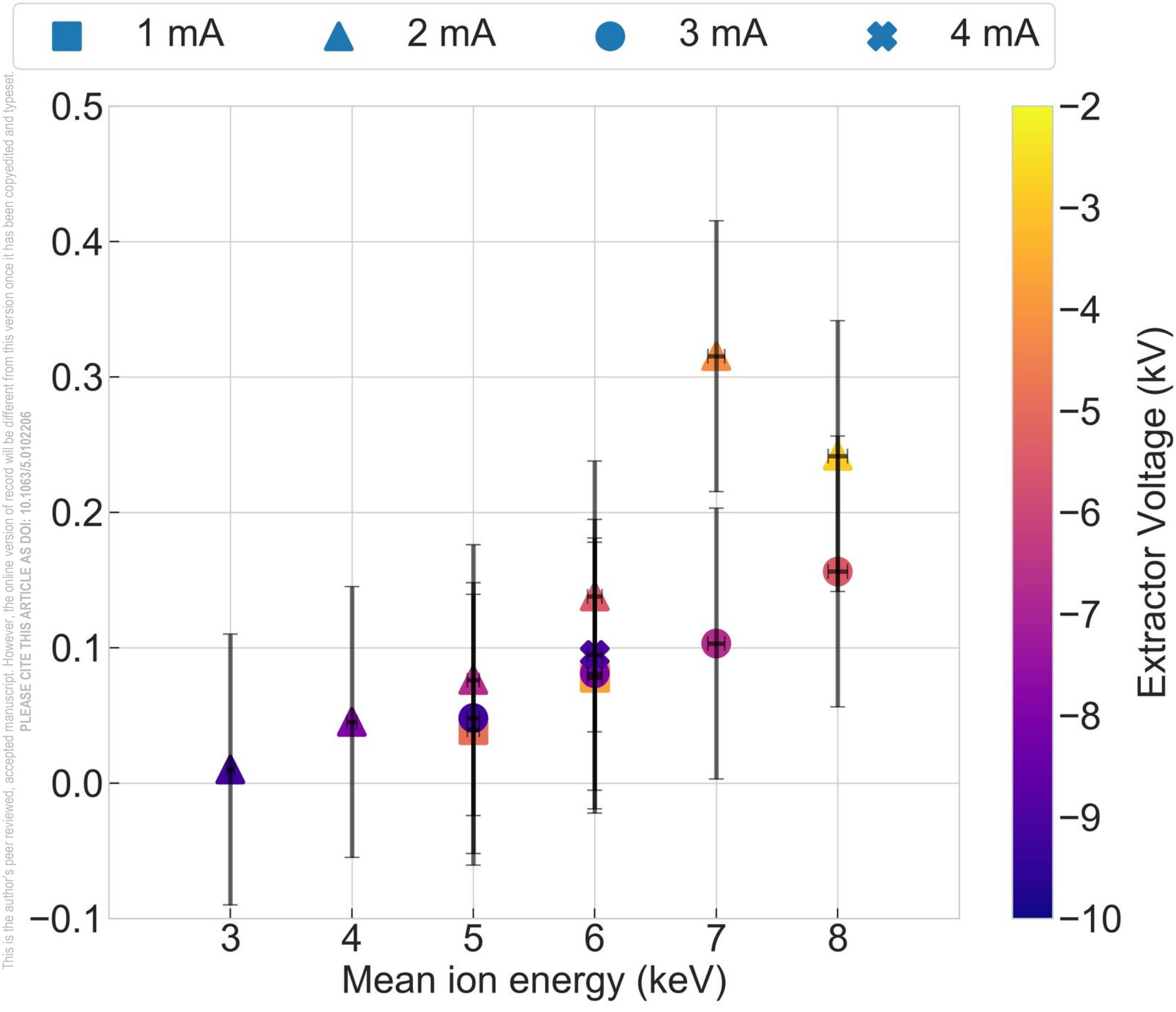

ACCEPTED MANUSCRIPT

Journal of Applied Physics

AIP Publishing

This is the author's peer reviewed, accepted manuscript. However, the online version of record will be different from this version once it has been copyedited and typeset.

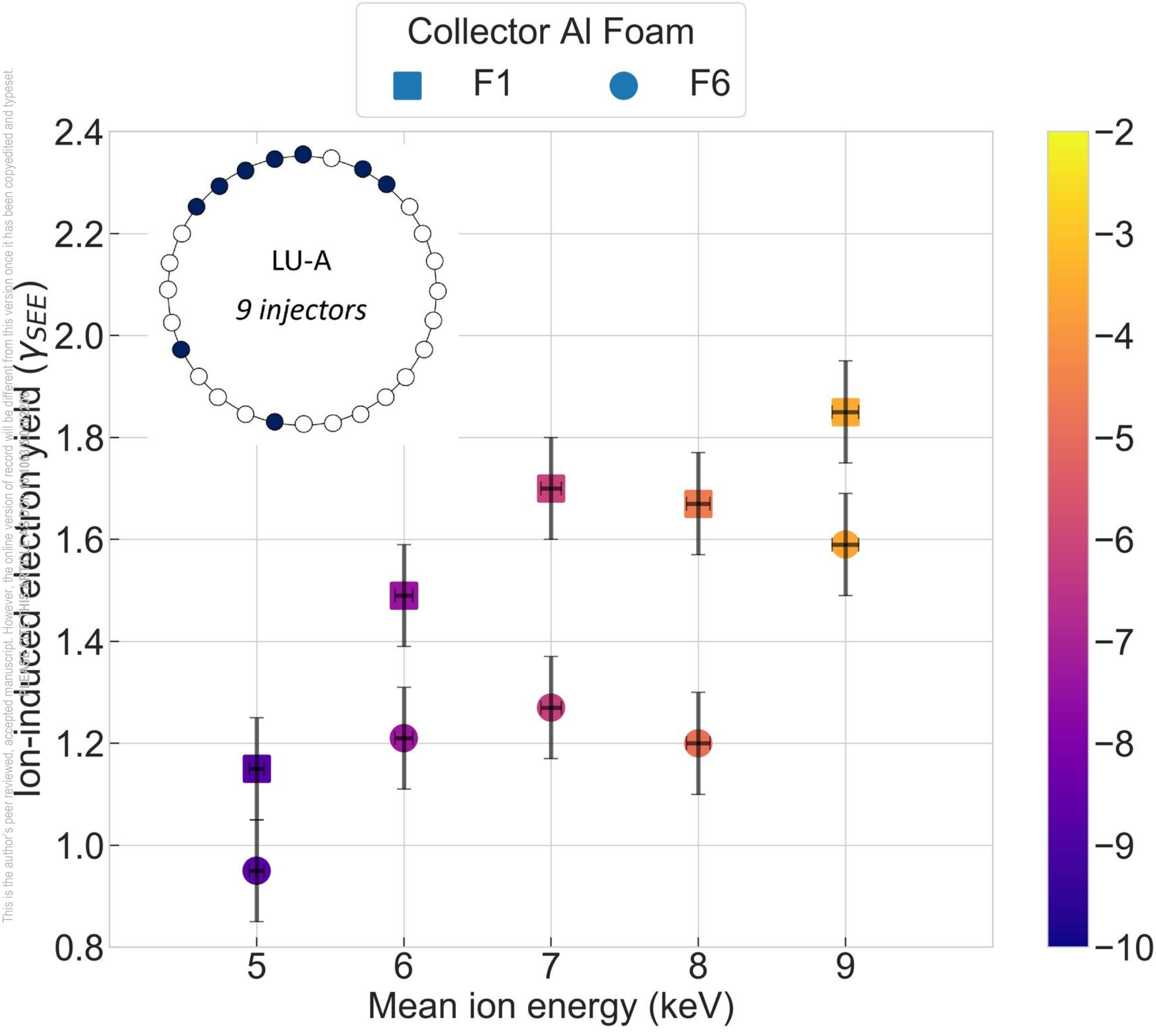

ACCEPTED MANUSCRIPT

Journal of Applied Physics

AIP Publishing

This is the author's peer reviewed, accepted manuscript. However, the online version of record will be different from this version once it has been copyedited and typeset.
PLEASE CITE THIS ARTICLE AS DOI: 10.1063/5.0102206

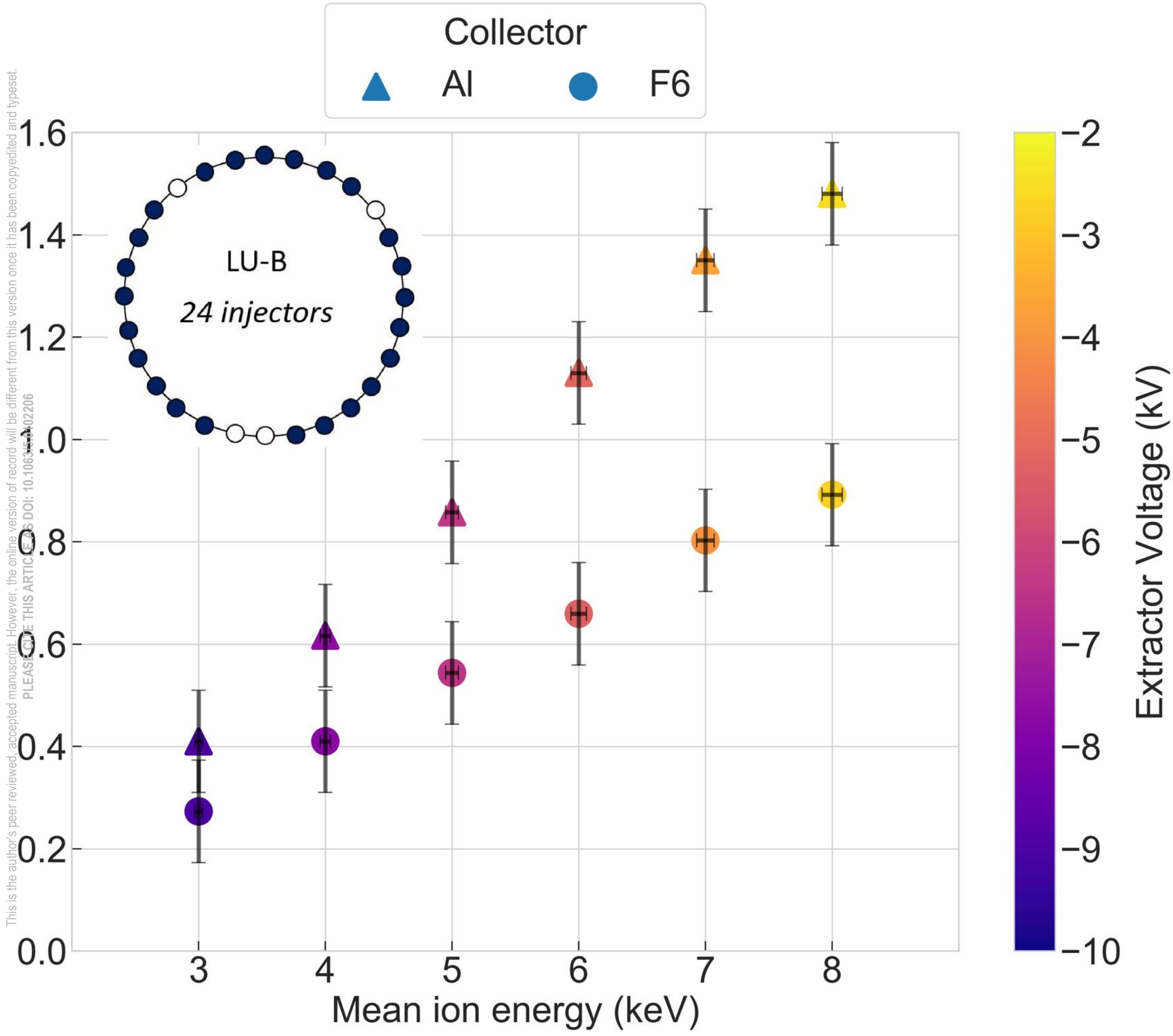

ACCEPTED MANUSCRIPT
Journal of Applied Physics
AIP Publishing
This is the author's peer reviewed, accepted manuscript. However, the online version of record will be different from this version once it has been copyedited and typeset.
PLEASE CITE THIS ARTICLE AS DOI: 10.1063/5.0102206

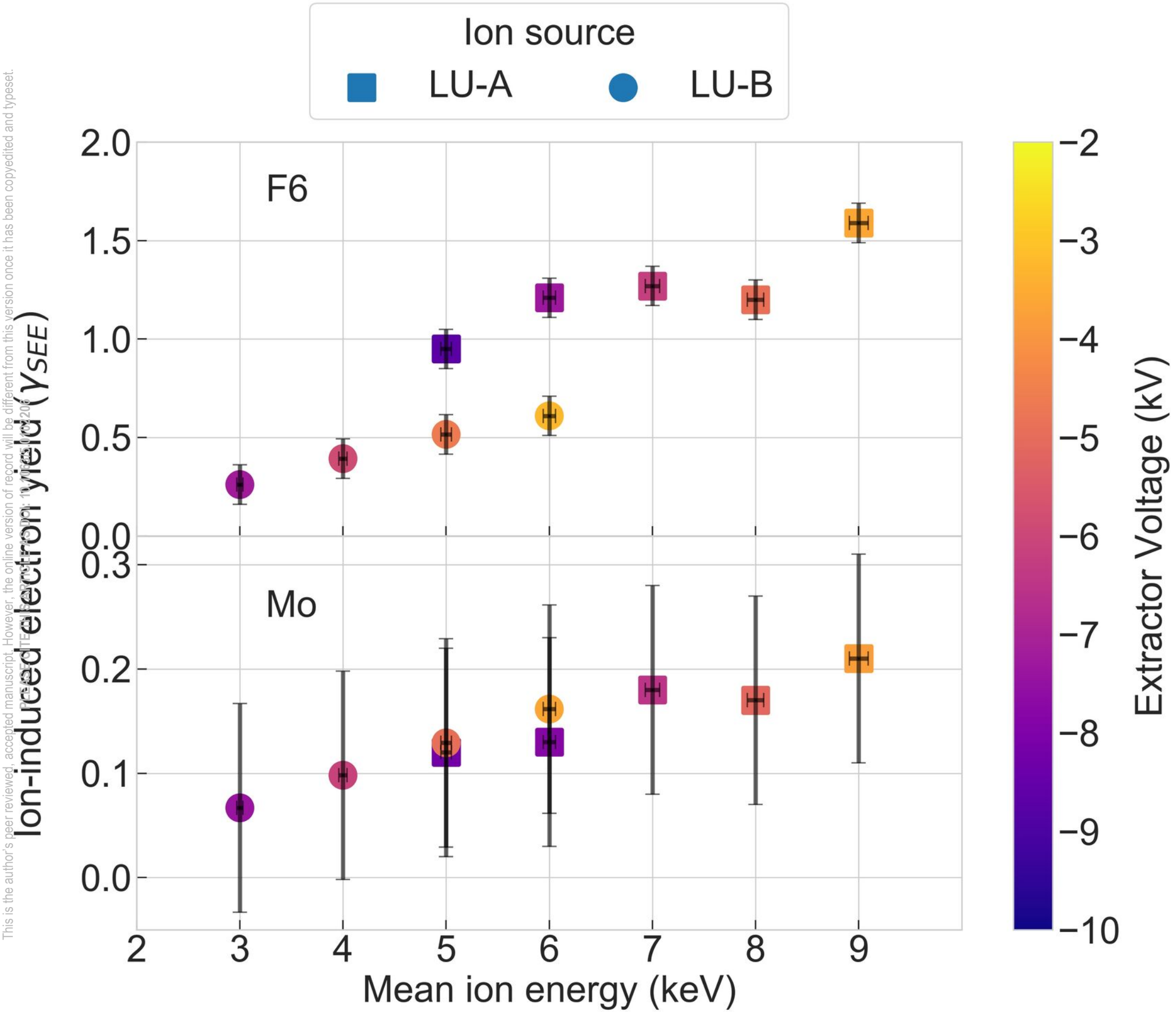

ACCEPTED MANUSCRIPT
Journal of Applied Physics
AIP Publishing
This is the author's peer reviewed, accepted manuscript. However, the online version of record will be different from this version once it has been copyedited and typeset.
PLEASE CITE THIS ARTICLE AS DOI: 10.1063/5.0202206

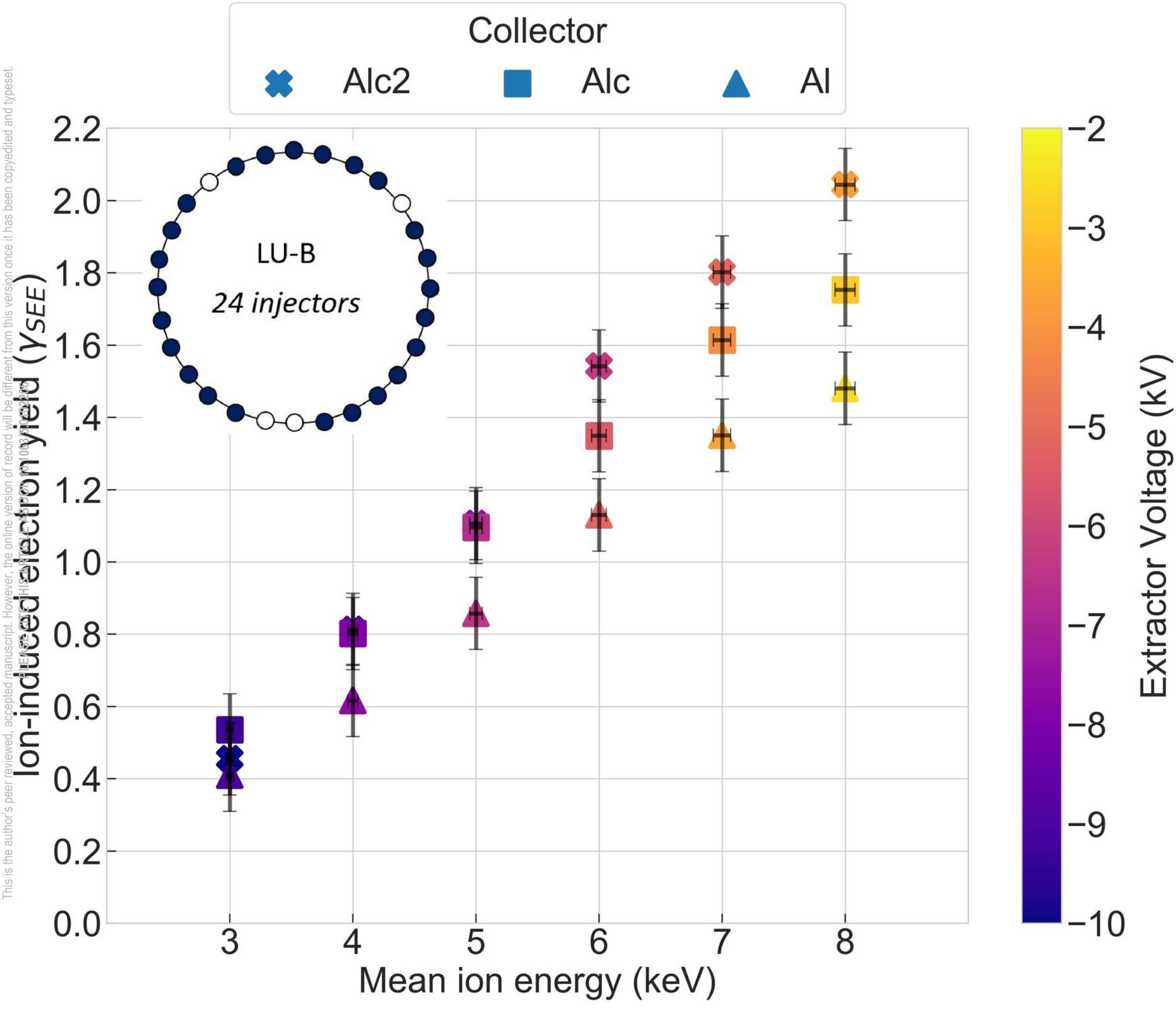

ACCEPTED MANUSCRIPT

Journal of Applied Physics

AIP Publishing

This is the author's peer reviewed, accepted manuscript. However, the online version of record will be different from this version once it has been copyedited and typeset.
PLEASE CITE THIS ARTICLE AS DOI: 10.1063/5.0072226

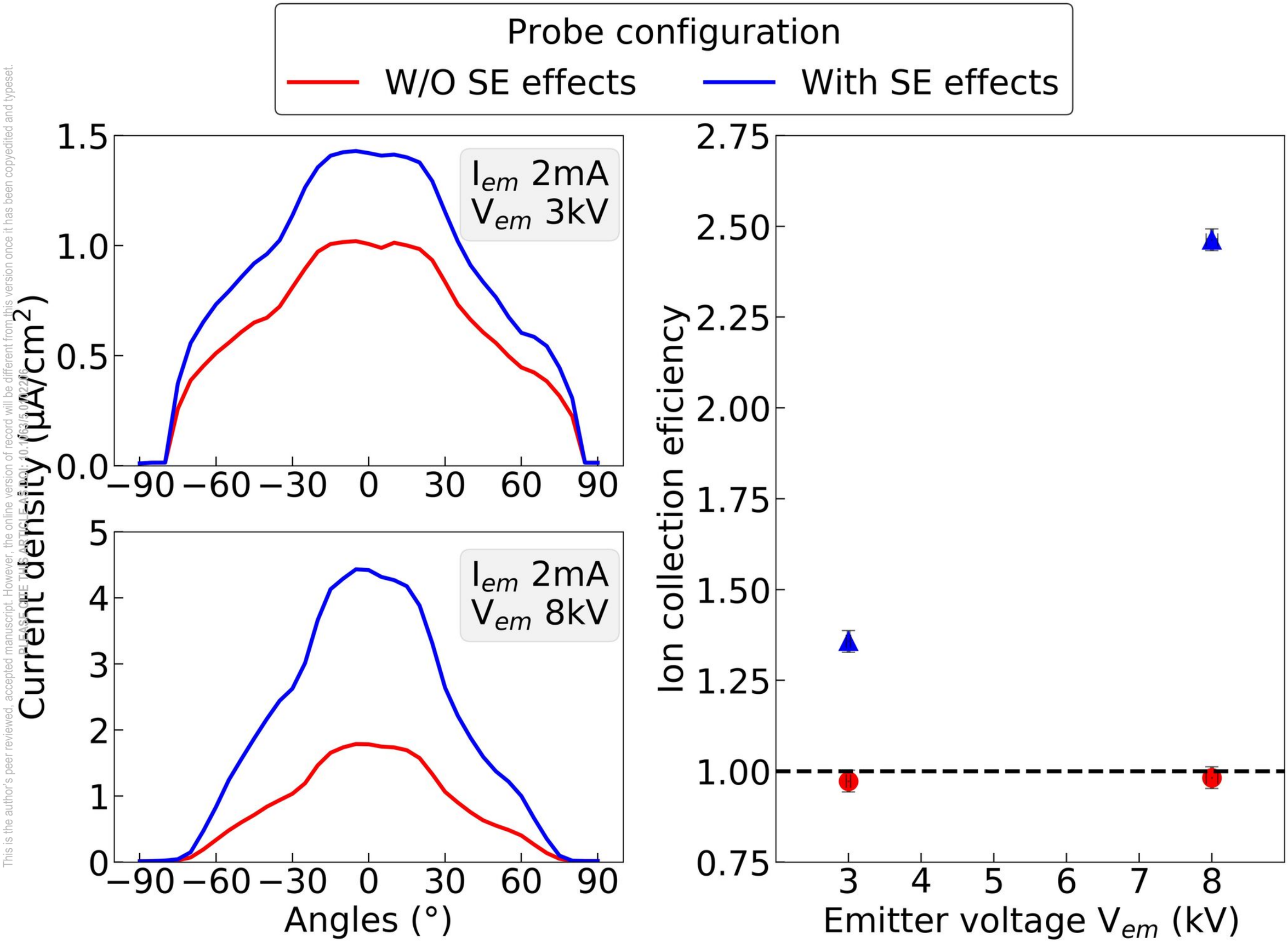

ACCEPTED MANUSCRIPT

This is the author's peer reviewed, accepted manuscript. However, the online version of record will be different from this version once it has been copyedited and typeset.
PLEASE CITE THIS ARTICLE AS DOI: 10.1063/5.0102206

Journal of Applied Physics
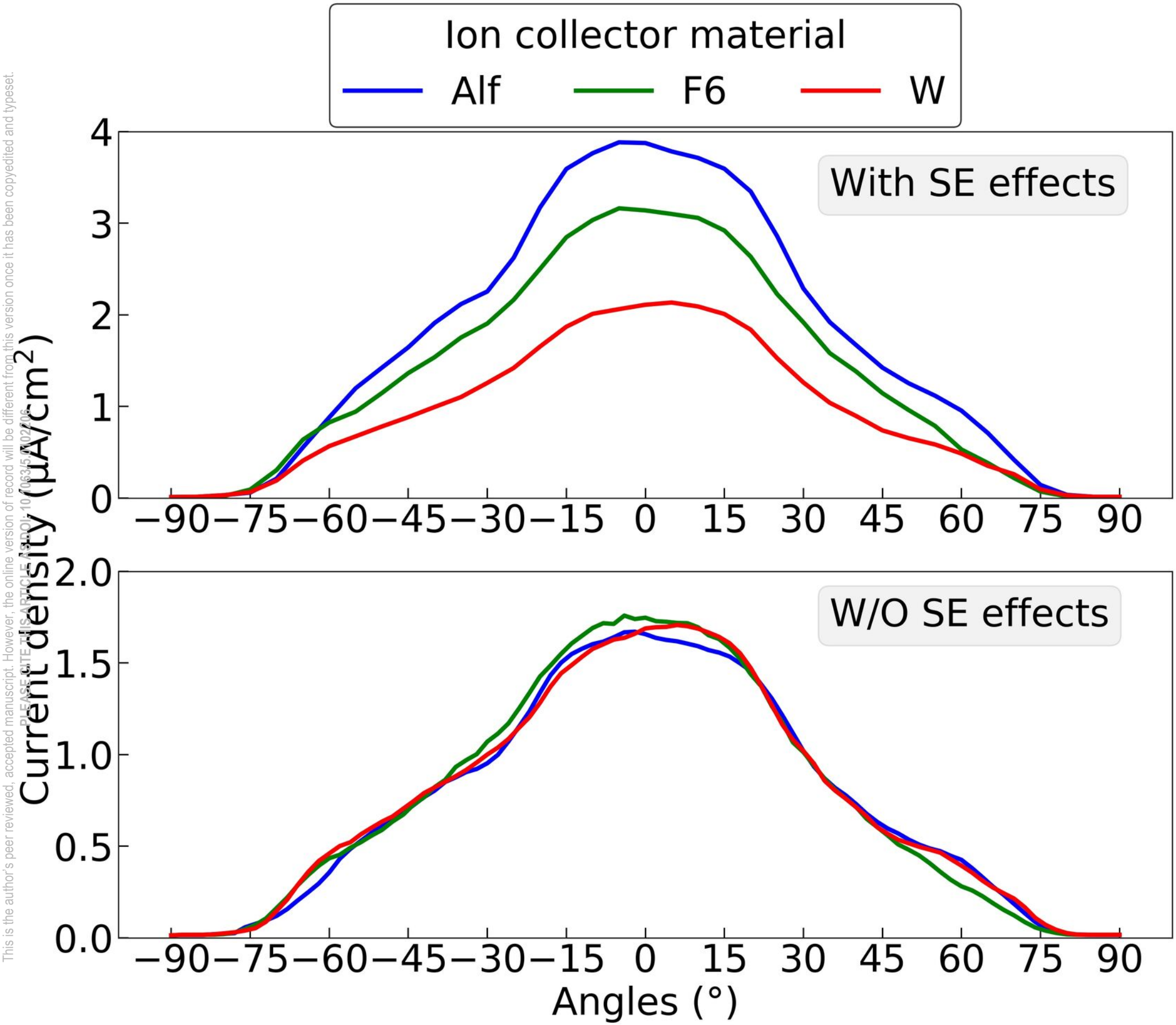
AIP Publishing